AN ABSTRACT OF THE THESIS OF

Renato Oscar Kowsmann for the Master of Science
(Name) (Degree)

in Oceanography presented on 27 October 1972
(Major) (Date)

Title: SURFACE SEDIMENTS OF THE PANAMA BASIN: COARSE COMPONENTS

Abstract approved: Redacted for Privacy

The abundance and distribution of biogenic, terrigenous and volcanic particles in the Panama Basin are markedly dependent on bottom topography and dissolution of calcite in the deeper parts of the basin. Of the coarse fraction ($>62\mu$), foraminiferal tests and acidic volcanic glass shards are concentrated on the Cocos and Carnegie Ridges as lag deposits. Foraminiferal fragments are found on these ridge flanks and on the Malpelo Ridge due to reworking by bottom currents accentuated by dissolution of calcite with increasing depth. The finest calcite, probably coccoliths with fine foraminiferal fragments, together with the hydrodynamically light radiolarian skeletons are concentrated by bottom currents in the basin adjacent to the ridges.

The foraminiferal calcite compensation depth in the basin is 3400 m. This relatively shallow depth probably reflects the high

surface water productivity over the basin, although the pattern of productivity is not reflected in the pattern of biogenic sediments.

Acidic volcanic glass appears to have been carried into the basin from Costa Rica, Colombia and Ecuador by easterly winds at altitudes of 1500 to 6000 m. Basaltic shards from the Galapagos Islands have been dispersed only over short distances to the west. Terrigenous sand-sized material is found on the edge of the continental shelf, where associated glauconite points to a relict origin, and along the northern Cocos Ridge, where contour currents may act as the dispersal mechanism.

Surface Sediments of the Panama Basin:
Coarse Components

by

Renato Oscar Kowsmann

A THESIS

submitted to

Oregon State University

in partial fulfillment of
the requirements for the
degree of

Master of Science

June 1973

APPROVED:

Redacted for Privacy

Associate Professor in Oceanography
in charge of major

Redacted for Privacy

Assistant Professor in Oceanography
in charge of major

Redacted for Privacy

Dean of the School of Oceanography

Redacted for Privacy

Dean of Graduate School

Date thesis is presented 27 October 1972

Typed by Marjorie Hay for Renato Oscar Kowsmann

ACKNOWLEDGEMENTS

I am deeply indebted to Drs. Ross Heath and Ted Moore, my major professors, for their guidance, encouragement and patience throughout all phases of this work. Their unorthodox approach to sedimentology will greatly influence me in my future work. They also made available their carbonate, opal and quartz data on the Panama Basin, which I used extensively in this work.

Drs. Don Pierce, Alan Niem and Christopher Bayne are thanked for their advice and for serving on my committee. Dr. Tjeerd van Andel, Dr. Ted Moore, Menno Dinkelmann and Bruce Malfait provided much of the supporting evidence for my conclusions. A timely pre-print of Dr. van Andel's paper on grain size was especially useful. Menno Dinkelman's helping hand with literature references is also acknowledged. Discussions with Dr. van Andel, Menno Dinkelman, Dave Ellis, Tim Baumgartner and Victor Rosato were extremely helpful. Nick Pisias, Ken Keeling and Dave Standley provided much needed advice on using the computer facilities. I also profited considerably from Ken Scheidegger's familiarity with volcanic glass shards. William Gilvert made the hydrographic data of YALOC-71 available in its reduced form. Margie Hay typed the manuscript and Anastasia Sotiropoulos drafted some of the figures. I sincerely thank them.

Due to the somewhat interdisciplinary nature of this work, I consulted many people from other fields of oceanography. Their suggestions were greatly appreciated, but, of course, I take responsibility for the conclusions.

Many of the samples used in the study came from the collections of Lamont-Doherty Geological Observatory and Scripps Institution of Oceanography.

The research was supported by the Office of Naval Research (contract N00014-67-A-0369-0007 under project NR 083-1021). Personal financial support was provided in part by Oregon State University's Foreign Student Scholarship fund, and by the Conselho Nacional de Pesquisas of Brasil.

Throughout my entire academic career, I have received the most enthusiastic support from my parents. This thesis is dedicated to them.

TABLE OF CONTENTS

LIST OF FIGURES

SURFACE SEDIMENTS OF THE PANAMA BASIN: COARSE COMPONENTS

INTRODUCTION

a) Background

In 1968, marine geologists from the Department of Oceanography at Oregon State University proposed a comprehensive study of deep-sea sediments in an effort to better understand the factors that control their distribution. The Panama Basin was chosen as a model area because of its variety of topographic features, complex water circulation, location within the high productivity belt of the equatorial Pacific and range of sediment sources.

The general distribution patterns of deep-sea sediments in the world oceans had already been described by numerous authors. Also, attempts had been made to relate these patterns to oceanic circulation, wind systems and bottom topography. Summaries are presented by Bramlette (1961), Arrhenius (1963) and recently Lisitzin (1972). Thus, the Panama Basin study evolved in order to look at a similar but smaller system in more detail in order to study the scale limits of the ocean-wide distributions, and the actual processes affecting deep-sea sediments.

The physiography and tectonism of the Panama Basin, which form the framework for the sedimentation study, have been described by van Andel et al. (1971a). The Panama Basin is bounded on the north by the Cocos Ridge, which extends southwest from the continental shelf of Costa Rica towards the Galapagos Islands to approximately 2° N (Figure 1). The southern limit of the basin just south of the equator, is formed by the Carnegie Ridge which trends east-west. The Galapagos Archipelago lies at the western end of this ridge. The continental margins of Costa Rica, Panama, Colombia and Ecuador close the basin on the east. Two other smaller topographic highs, the Coiba and the Malpelo Ridges, split the basin longitudinally into an eastern basin which is generally deeper than 3200 m and a western basin ranging from 2200 m to 3200 m deep. The Coiba Ridge is attached to the continent at its northern end whereas the Malpelo Ridge is an isolated block. The east-west trending spreading center called Galapagos Rift Zone has no marked topographic expression but is distinguished by a total lack of sediment cover. The north-south trending lineations in the topography of the basin reflect the fracture zone pattern shown by van Andel et al. (1971a). Although the Yaquina Graben forms a topographic depression in the eastern basin, no trenches are found within the study area. The Mid-America Trench terminates against the Cocos Ridge, and the Peru-Chile Trench meets a similar fate as it reaches the Carnegie Ridge. Consequently, no active subduction of the ocean floor is evident in the Panama Basin (van Andel et al., 1971a).

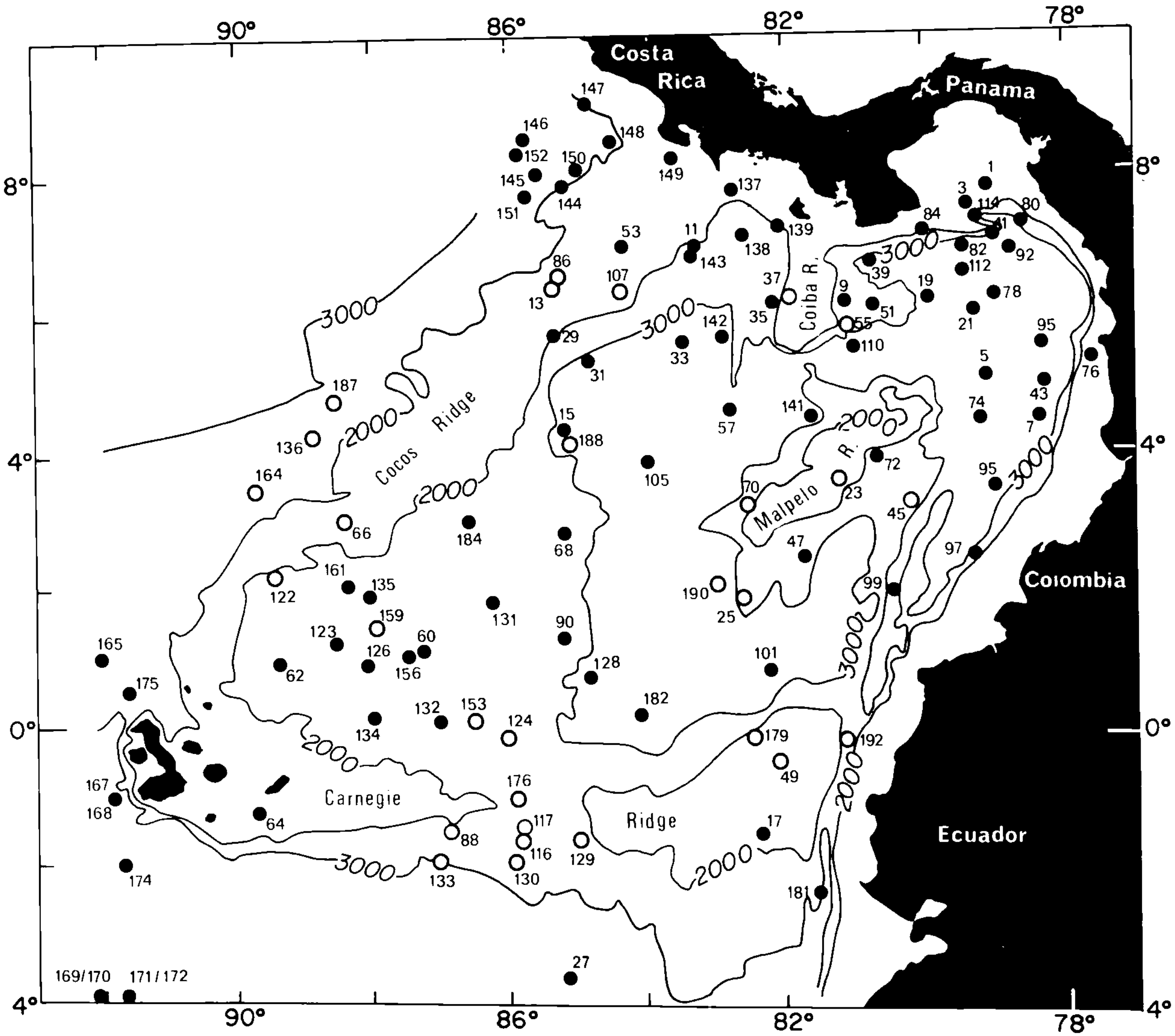

Figure 1. Location of surface samples. Open circles represent samples containing reworked microfossils. Contours in meters.

The main effects of the topography on the general sediment distribution have been evaluated by Moore et al. (1973, in press). Most of the terrigenous material is confined to the low lying areas of the eastern basin. Consequently, the isolated ridges and the western basin receive almost exclusively biogenic sediments. This fractionation can be seen in the grain size distribution maps of van Andel (1973, in press). Fine sediments ($<62\mu$) are most abundant in the deep parts of the eastern basin, whereas coarse sediments occur on the ridges and in the western basin. Terrigenous sediments consist mostly of clays, whereas the biogenic sediments are formed predominantly by sand sized tests of planktonic foraminifera and radiolaria. Detrital mineral sands are found on the edge of the continental shelf and on the slope. Volcanic glass shards are found on the Cocos and Carnegie Ridges.

b) Purpose of the Study

The relative abundance of biogenic phases in deep-sea sediments is primarily a reflection of the balance between rates of supply and rates of removal. Near continental margins, the influence of dilution by terrigenous material also becomes important. The rate of supply is mostly a function of productivity, whereas the rate of removal depends upon chemical and physical properties of the bottom waters that act on the sediment. Both solution and winnowing remove sediments.

In addition, in situ reworking helps expose soluble tests to corrosive bottom waters and thereby increases the rate at which they dissolve.

To better understand the processes that modify the primary depositional patterns of deep-sea sediments, it is necessary to determine the response of various components of the sediment to a range of environmental conditions. The coarse fraction ($>62\mu$) in Panama Basin sediments contains grains of biogenic calcite and opaline silica as well as terrigenous minerals. Because microscopic examination of this size fraction reveals subtle changes in the character of the particles, as well as in their abundance, it has been chosen in preference to the more abundant finer fractions for detailed study. In addition, coarse terrigenous debris is rarely abundant enough to mask the effects of dissolution and reworking on sand-sized biogenic particles, a state of affairs that is not true for finer fractions in samples collected near the continental margin. Hydrodynamically, some of the particles retained on a 62μ sieve behave as silt grains, thereby increasing the effective size range studied.

Under current action foraminifera should be less easily eroded than radiolaria because the latter consist of an open meshwork of opaline silica, often with protruding ornamentation, that renders them hydrodynamically light. Studies by Berger (1971) have revealed that most foraminiferal tests suffer drastic dissolution after deposition. In the course of dissolution, the calcareous tests commonly break up.

The fragments are probably more succeptible to transport than the whole foraminifera. Thus, to evaluate the relative roles of dissolution and reworking on biogenic particles, whole foraminifera, foraminiferal fragments, and radiolaria have been distinguished throughout the study.

The value of glass shards as a tool for tracing sources and dispersal of deep-sea sediments has been recognized for some time. Thus, Ninkovich _et al._ (1964) determined that volcanic ash layers cored in the vicinity of the Mid-Atlantic Ridge came from the South Sandwich Islands some 750 km away, and Horn _et al._ (1969) defined the source areas of the various types of ash layers throughout the North Pacific on the basis of color and grain size of the glass shards. In the Panama Basin, three types of glass shards are present in the coarse fraction. The distribution of these types provides information on the source areas and paths of dispersion of non-biogenic components of the sediments.

Although this is a self-contained study, its results complement the independent investigations of the grain size (van Andel, 1973, in press), distributions of all biogenic components (Moore _et al._, 1973, in press) and mineralogy (Heath _et al._, 1973, in press) of Panama Basin sediments.

c) Oceanographic Setting

The surface circulation of the Panama Basin has been described by Wooster and Cromwell (1958), Wyrtki (1965) and Stevenson (1970). In brief, it is the meeting place of the Peru Current with the North Equatorial Countercurrent. Local wind-driven circulation generates small gyres within the basin, exemplified by the Colombia Current. Except where it produces upwelling, the surface circulation has little influence on bottom sediments.

Laird (1971) deduced the bottom circulation by means of potential temperature changes. On the basis of data collected during YALOC-71 as well as the data available to Laird (Appendix V), and using the much improved bathymetric chart published by van Andel et al. (1971a), it has been possible to develop the new map of bottom water flow shown in Figure 2. It mainly confirms the broad features described by Laird (1971) but differs in detail, mainly due to better topographic control. The bottom waters enter the basin through the Peru-Chile Trench, circulate around the Malpelo Ridge and spread towards the western basin, warming up considerably along the way. Recently, Lonsdale et al. (1972b) reported the presence of ripple marks and dunes of foraminiferal sand along the gap in the central Carnegie Ridge. Similar structures on Horizon Guyot were produced by tidal currents of velocities exceeding 15 cm/sec (Lonsdale et al.,

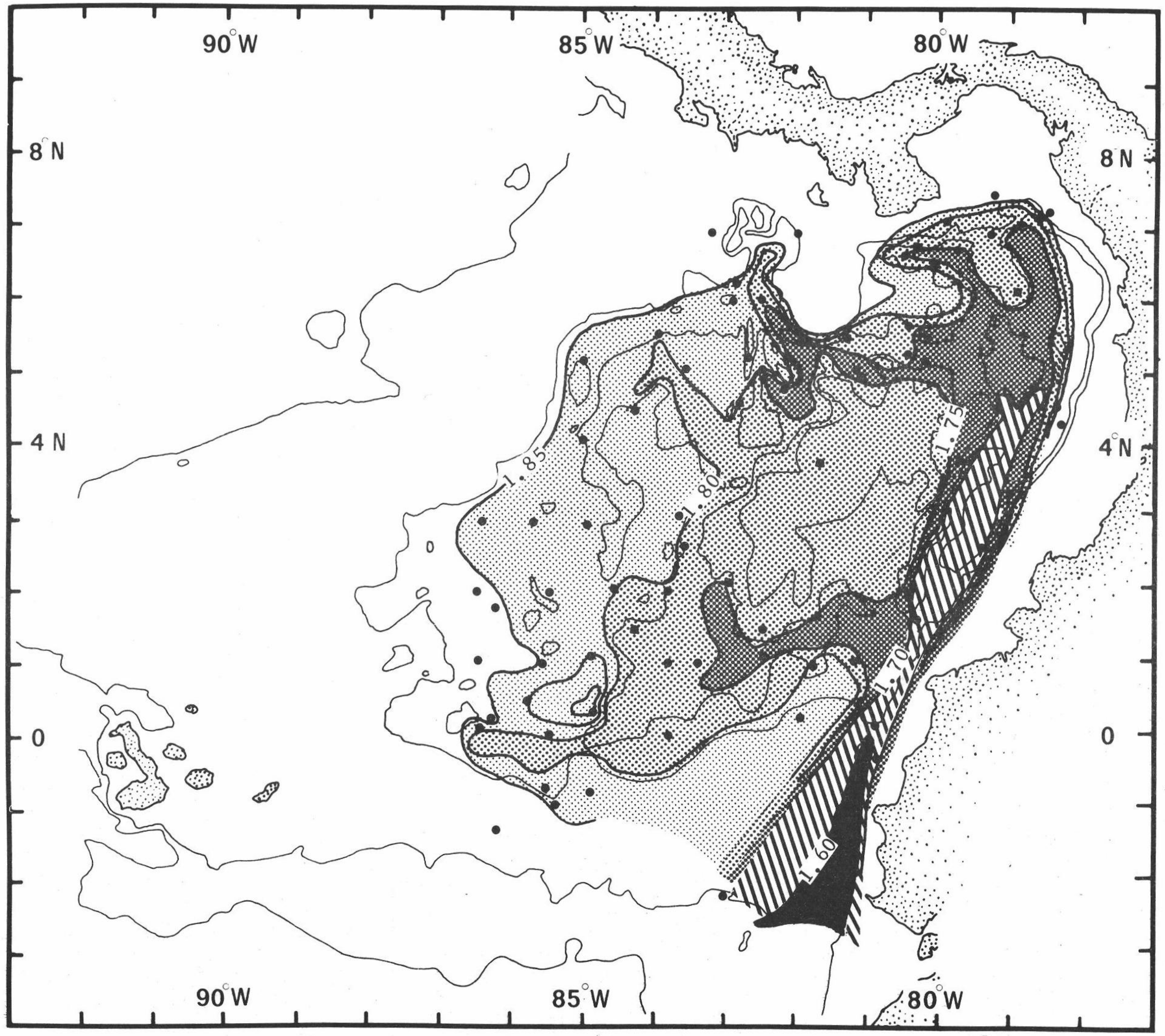

Figure 2. Bottom water circulation in the Panama Basin, modified after Laird (1971). Potential temperature contours are in centigrade degrees. Black dots represent stations.

1972a). Indirect evidence for strong current activity on the ridges existed prior to this study. Van Andel et al. (1971a) found sediment thicknesses of 600 meters both north and south of the Carnegie Ridge, whereas basaltic basement and Miocene cherts were exposed in the central saddle at the ridge crest (van Andel et al., 1971b). Slightly thinner sediments surround the Cocos Ridge, but again contrast with the sediment-free ridge crest. Both T. Moore and M. Dinkelman (personal communication, 1972), using micropaleontologic evidence, conclude that most ridge sediments are reworked. Recently, van Andel (1973, in press) has further shown that winnowing is pronounced on the ridges, resulting in the transport of finer material down the ridge flanks.

It is possible that tidal currents, with their cyclic reversals of flow are responsible for most of the winnowing. This might be superimposed, however upon an advective current system, resulting in a net transport in or out of the basin across the ridges. In order to detect net flow across the ridges, sections of potential temperatures and potential densities have been constructed. The hydrographic data collected during YALOC-71 and the data provided by the NODC, were taken over many years. For the location of the hydrographic stations, see Appendix VI. Processing of the data is described in Appendix VII. Stations were chosen to span gaps across the Cocos and Carnegie Ridges. Locations of the sections are shown in Figure 3 together with

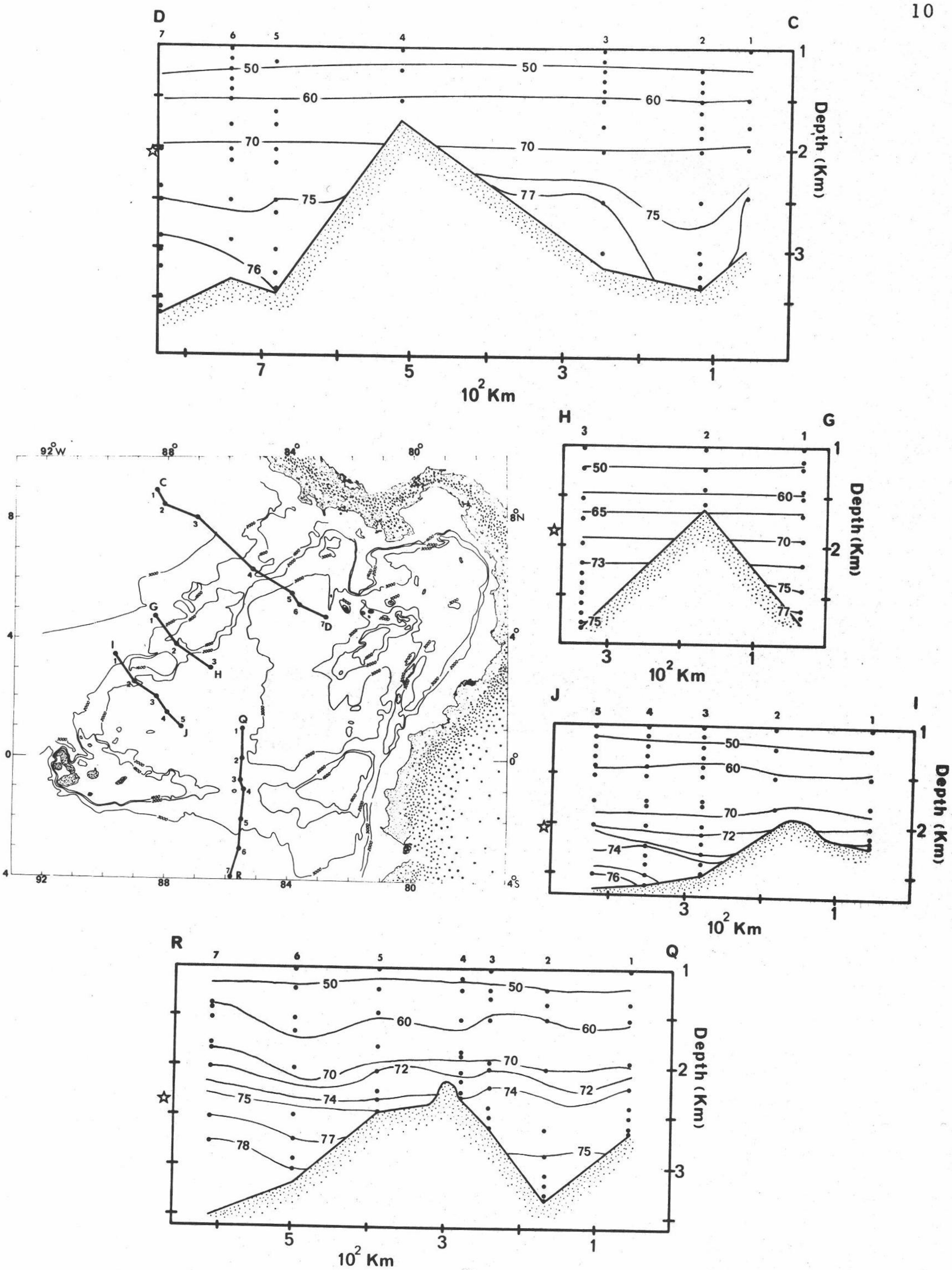

Figure 3. Hydrographic sections through saddles in the Cocos and Carnegie Ridges. Contours are (potential density - 27) x 100; i.e. 50 = 27.50. The star on the left side of each section marks the true sill depth for the gap. Control points are shown by black dots.

the potential density cross sections. One hoped that the constricted flow through the gaps would maximize current velocities, making flow patterns easier to detect. Most of the features in Figure 3 can also be observed in potential temperature sections suggesting that salinity exerts little effect on the potential density.

Regardless of location, potential density gradients are much greater outside than inside the basin, especially near the bottom. In all Cocos Ridge transects, density contrasts disappear at sill depth or slightly below it. On the Carnegie Ridge, the contrast extends above sill depth.

Across the Cocos Ridge, only section (IJ) indicates any preferential direction of flow. This transect shows slight downbending of the isopycnals inside the basin, suggesting water penetration into the basin. Transect (CD) shows very irregular density below sill depth. Although the data originate from several cruises, the regularity of the isopycnals above sill depth speaks against systematic measurement errors between institutions. Section (GH) shows no obvious trends.

Section (QR) on the Carnegie Saddle provides the most positive indication of net flow. In this section, the undulation of the potential density isopleths, and their downbending outside the basin point to both vertical mixing and outflow of water from the basin. Laird (1971) suggests that the Carnegie Saddle provides the route of escape of basin waters into the open sea. Because five stations out of six in section (QR) were occupied during Leg 4 of YALOC-71, his arguments are much less conclusive than those presented here. Sediment thicknesses seem to reflect these directions of flow. The isopach map of van Andel et al. (1971a) shows thickened sediments south of both the Cocos and the Carnegie Ridges.

d) Methodology

One hundred and fourteen surface samples were taken from short gravity and in some cases, piston cores (for sample locations see Figure 1 and Appendix I). These were wet-sieved through a 62 micron mesh. The retained coarse fraction was dried and split. One split, mounted with Canada Balsam, was termed the "carbonate slide." It contained all coarse components of the sediment. The other split was warmed in buffered acetic acid (pH = 5) until all the calcium carbonate was removed. After washing and drying the residue was mounted with balsam. It is identified as the "carbonate-free" slide. All grains were counted on both slides, totals in each ranging from 300 to 8000. On the average, counts reached more than 1000 grains per slide (for further details, see Appendix IV).

The following components of the carbonate slide were counted: whole planktonic foraminifera, fragments of planktonic foraminifera, radiolarian skeletons, minerals and benthic foraminifera (see

Appendix II).

More detailed counts were made of the remaining components in the carbonate-free slide. The radiolaria were subdivided into two sub-classes, Nassellaria and Spumellaria. The reason for this distinction was a suggestion by Haeckel (1887) that Nassellaria live in abyssal depths while Spumellaria are usually found very near the surface.

The minerals were also subdivided. Two types of shards were readily identified and counted. One consisted of brown (caramel colored) glass and the other consisted of colorless (transparent) glass.

Anisotropic, non-opaque minerals were also counted, as were glauconite grains, diatoms and sponge spicules.

In summary, Nassellaria, Spumellaria, brown volcanic glass shards, colorless volcanic shards, anisotropic non-opaque minerals, glauconite, diatoms and sponge spicules, were counted as components of the carbonate-free slides (see Appendix II). The data from the carbonate slides were converted to percentages of total coarse fraction (Appendix IIIa). Values for the carbonate-free slides were transformed into percentages of carbonate-free coarse fraction (Appendix IIIb).

SEDIMENT DISTRIBUTION

Once the percentages of each component in all samples were obtained, they were plotted on a Panama Basin base map for contouring. The results are discussed below. Only the maps that bear on the original goals of the study are presented here.

a) Distribution of Spumellaria and Nassellaria

No systematic difference in the abundances or distribution of Nassellaria and Spumellaria was detected. Spumellaria are invariably far more numerous than Nassellaria, with the ratio ranging from 28 : 1 to 3 : 1. There is a slight indication that the Spumellaria to Nassellaria ratio increases towards the continental margin. It ranges from 5 : 1 in the middle of the basin to 20 : 1 at the edge of the continental shelf. This is somewhat in agreement with Haeckel's hypothesis, but one must be cautious as the continental shelf samples contain few Radiolaria and counting statistics are therefore unreliable.

These results seem to confirm Campbell's ideas (1954), that although some Nassellaria live in abyssal depths, most are found together with Spumellaria in near-surface waters.

b) Distribution of Radiolaria "carbonate-free" (Figure 4)

Few radiolarians are found near the continental margin and

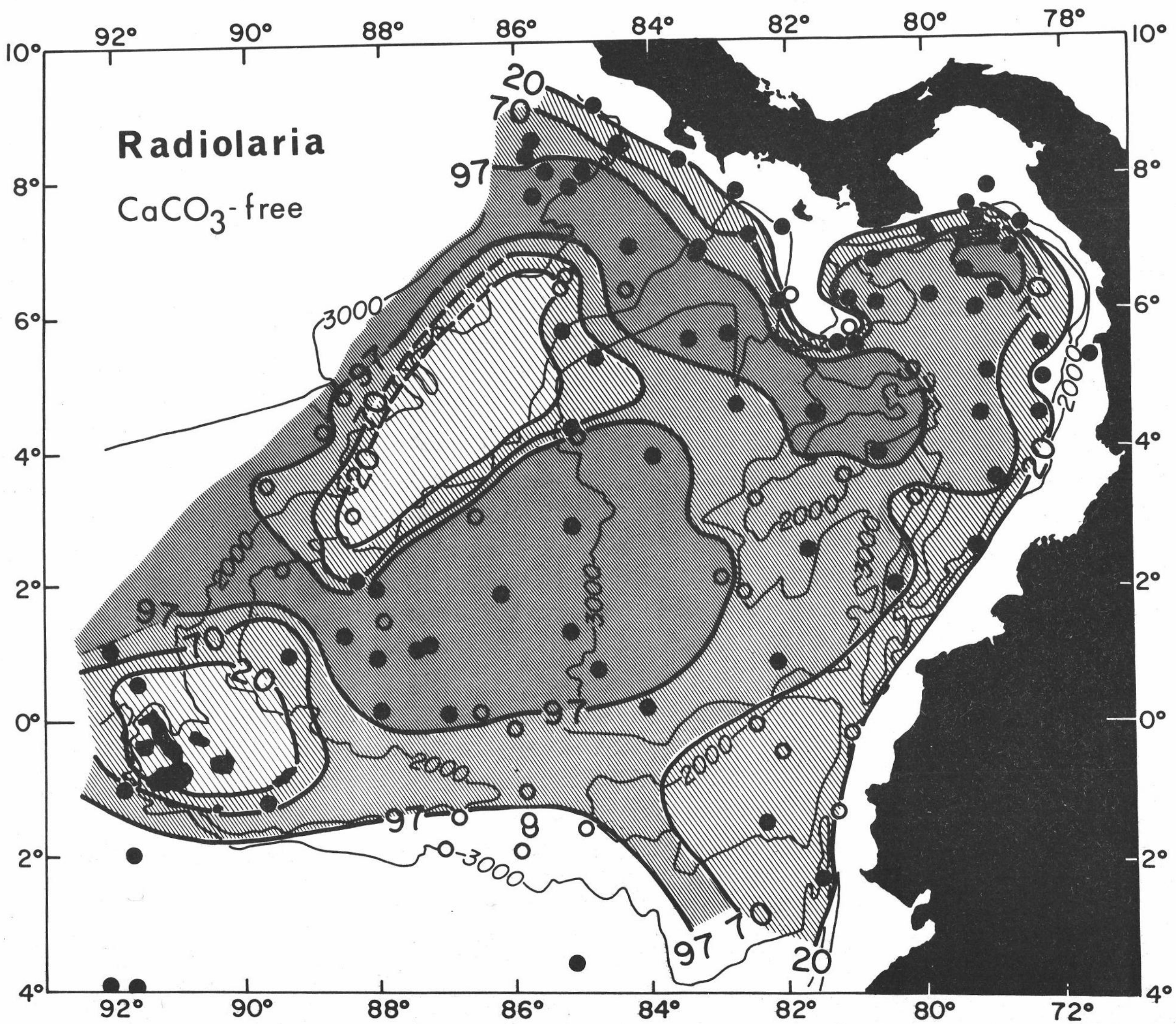

Figure 4. Distribution of radiolaria in surface sediments (carbonate-free coarse fraction). Open circles as Figure 1.

around the Galapagos Archipelago due to dilution by coarse terrigenous material and eroded volcanic debris, respectively. Areas of low abundance also coincide with the tops of the ridges.

Radiolarians are abundant in sediments of the shallow western basin, forming a pool between the surrounding ridges. They are also abundant in the eastern basin. This pattern is identical to the opal distribution described by Moore et al. (1973, in press), if one ignores the diluting effect of terrigenous clays near the continental margin.

The generally low concentration of radiolarians in ridge samples could reflect either silica dissolution at shallow depths or mechanical removal of the skeletons by ocean currents. M. Dinkelman (personal communication, 1972) reports that the preservation state of the radiolaria on the ridges is moderate to poor, but that even worse preserved assemblages are found in the deep eastern basin. This seems to indicate that pure dissolution is not the controlling factor. The evidence for vigorous current action on the ridges, presented in the previous chapter on physical oceanography, and the susceptibility of radiolarian skeletons to bottom transport suggest that the relative deficiency of radiolaria on the ridges is caused by current winnowing.

While winnowing from ridges seems to be responsible for some of the high concentrations of radiolaria in the western basin (normal pelagic sedimentation away from terrigenous influx provides additional contributions), we cannot use it to explain equally high concentrations in the eastern basin. Upwelling and high productivity must be involved.

Ellis (1972) has shown that in the South Atlantic surface standing crop is correlated with the opal content of sediments. Moore _et al_. (1973, in press) have tried to relate productivity (expressed as mg C/m^2/day) within the basin to the distribution of opal and radiolaria. Unfortunately, no clear correlation was found. The highly corroded radiolarian skeleton assemblages found in the eastern basin by M. Dinkelman (personal communication, 1972) suggest that their distribution is affected by bottom transport.

c) _Distribution of Radiolaria in Total Coarse Fraction_ (Figure 5)

Because of the negative correlation inherent in percentage data (Chayes, 1960), Figure 5 is essentially the complement of the combined foraminiferal maps. The tongue of abundant radiolaria extending south near the continental margin marks the location of the Yaquina Graben. This topographic feature is isolated from the continental margin by a sill 2400 m deep. This sill blocks off coarse terrigenous sediments. Since the graben is too deep for carbonate deposition, radiolarians are the only coarse particles that reach the sea floor.

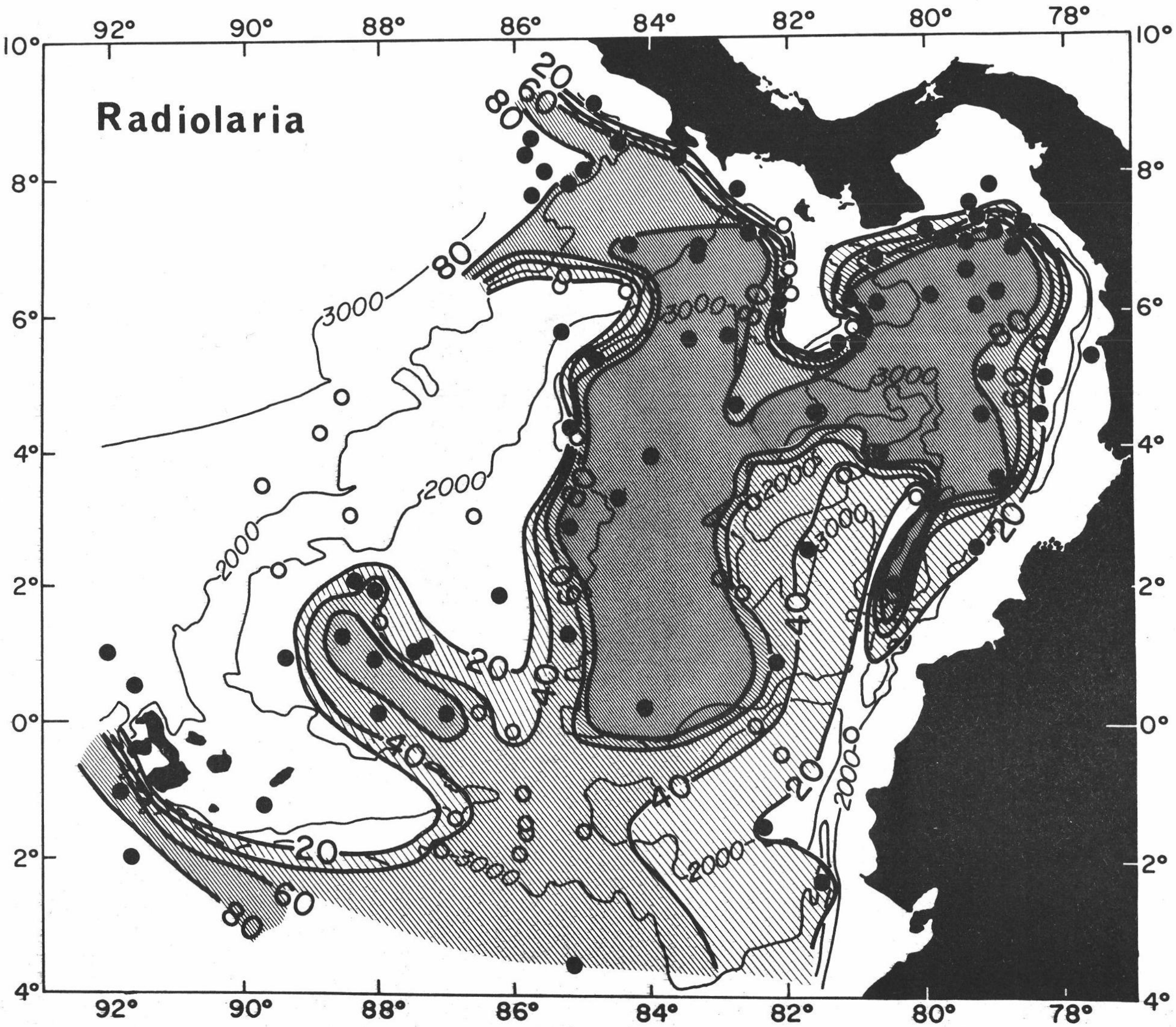

Figure 5. Distribution of radiolaria in surface sediments (percent of total coarse fraction).

d) Distribution of Whole Planktonic Foraminifera (Figure 6)

Whole foraminifera are very abundant in ridge sediments, especially those on the Galapagos pedestal of the Carnegie Ridge. The pattern closely resembles the carbonate distribution presented by Moore *et al.* (1973, in press). The only exception is the Malpelo Ridge, where carbonate-rich sediments are present, but whole foraminifera are conspicously lacking. This apparent deficit is accounted for by the abundance of foraminiferal fragments and fine carbonate.

The abundance of whole foraminifera on the ridges emphasizes the considerations of the previous sections. Selective sorting removes radiolarians while coarser and hydrodynamically larger foraminiferal sand is left behind. The continental margins, where a similar process might be expected, are low in whole planktonic foraminifera due to dilution by mineral grains.

Low foraminiferal values on the eastern basin can be attributed to the dissolution of calcium carbonate with depth. The calcite compensation depth (Bramlette, 1961) in the Panama Basin is 3400 meters (Moore *et al.*, 1973, in press). The hydrographic data outlined previously (Figure 2) show that the coldest and most corrosive bottom water circulates first through the eastern basin. By the time it flows into the carbonate-rich western basin, it has warmed up considerably.

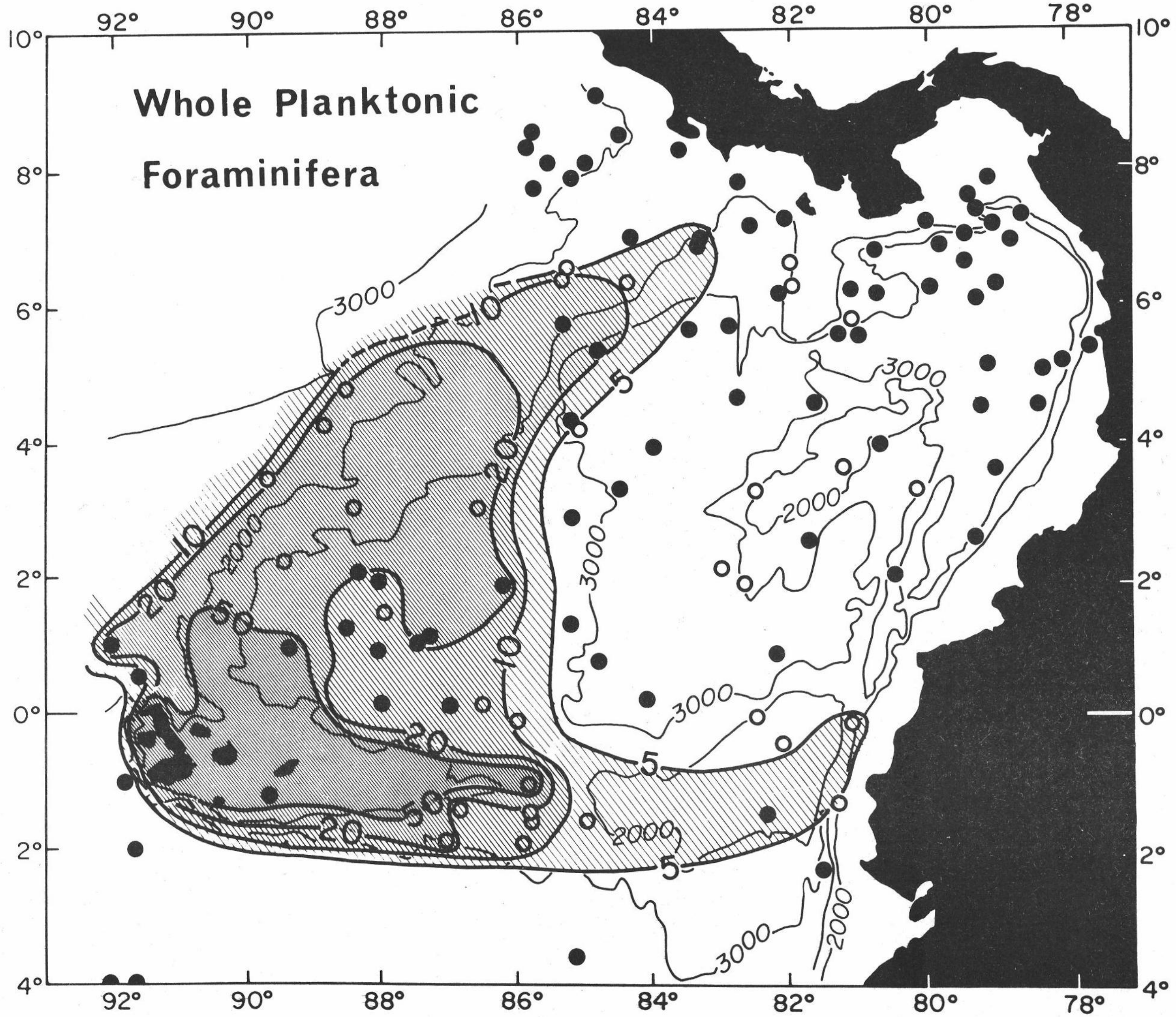

Figure 6. Distribution of whole planktonic foraminifera in surface sediments (percent of total coarse fraction). Open circles as Figure 1.

e) Distribution of Planktonic Foraminiferal Fragments (Figure 7)

The concentration of foraminiferal pieces is high on the slopes of all four major ridges, although the pattern is least well defined on the Carnegie Ridge. The concentration is low on the ridge crests, where whole foraminifera predominate. As with the whole foraminifera, fragments are absent in the eastern basin.

The restriction of fragments to the flanks of ridges at intermediate depths can be explained by either partial dissolution of whole tests with increasing depth, or by reworking processes, which, in addition to exposing the tests to dissolution, would tend to remove the smaller pieces depositing them downslope. The mean percentage of foraminiferal fragments within the coarse fraction of the 28 reworked samples identified by Moore is 50%. On the other hand, the mean for all other samples is only 18%. This suggests that mechanical reworking and resultant increased exposure to attack by corrosive bottom waters is an important factor in the fragmentation of foraminiferal tests.

Reworking must be especially vigorous on the Malpelo Platform because essentially all foraminifera have been reduced to fragments. The proximity of cold, corrosive bottom waters, the steepness of the slopes and the constriction caused by the ridge, increasing current velocities as they swing west, create an especially harsh environment

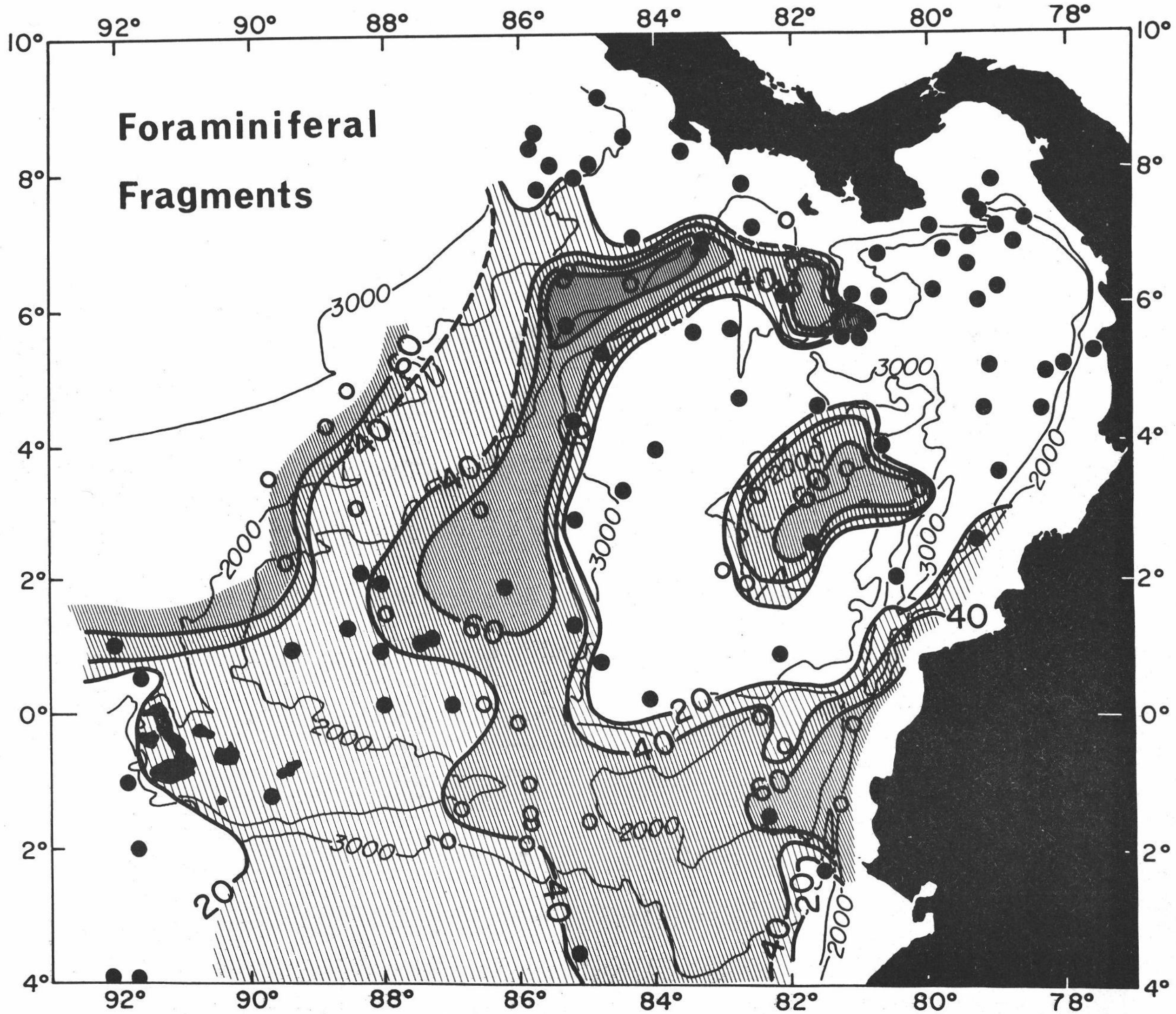

Figure 7. Distribution of planktonic foraminiferal fragments in surface sediments (percent of total coarse fraction). Open circles as Figure 1.

for the survival of carbonate shells. The presence of radiolaria on the north slopes of the Malpelo Ridge suggests that erosion by bottom currents is minimal there and points to the important role played by dissolution in the comminution of foraminifera.

The north Cocos Ridge area is anomalous. As already mentioned, unlike other parts of the ridge, it contains abundant radiolaria. Furthermore, it contains few foraminiferal tests (either whole or broken). Dilution by terrigenous sand grains is not a logical explanation since radiolaria dominate the coarse fraction. Winnowing can be excluded since the samples on the north Cocos Ridge show no micropaleontologic evidence of reworking, and since the hydrodynamically light radiolaria are not depleted. In upwelling areas like the Panama Basin which are adjacent to continents, the production of organic matter seems to outweight the production of foraminifera (Parker and Berger, 1971). In the Panama Basin, both algal blooms and continental detritus are important sources of organic matter (Forsbergh, 1969). As a result, benthic activity in such areas is high and corrosive bottom waters are present at quite shallow depths, leading to a marked shoaling of both the lysocline and the calcite compensation depth. There is no evidence for upwelling on the north Cocos Ridge (Moore _et al._, 1973, in press). Therefore, highly corrosive conditions may be present near the bottom without the high production of calcareous tests in the overlying waters. The result is a scarcity of calcareous sediments in the area.

In contrast with the north Cocos Ridge, marked upwelling and high productivity occur over the eastern Carnegie Ridge (Moore *et al.*, 1973, in press). Here surface sediments contain abundant foraminiferal tests. These differences cannot be quantitatively evaluated by the sediment data available in this study. However, it is clear that even though bottom waters on both the Cocos and the Carnegie Ridges are rich in CO_2 and are highly corrosive to calcite (Culberson, 1972), the rate of supply of foraminifera to the Carnegie Ridge exceeds the rate of solution while on the Cocos Ridge it does not.

f) Distribution of Fine Carbonate (Figure 8)

The concentration of calcium carbonate in the fine ($<62\mu$) fraction of Panama Basin sediments was calculated by subtracting the percent weight of foraminifera in the $>62\mu$ fraction from the percent weight of carbonate in the total sediment (Moore *et al.*, 1973, in press). The data on carbonate in the total sediment are expressed as weight percents, whereas those for foraminifera (whole forams + fragments)[4] are expressed as numerical percents. The latter must be converted to weight percents on the basis of the weight of an average grain of each coarse component. The following grain masses were used in the calculation:

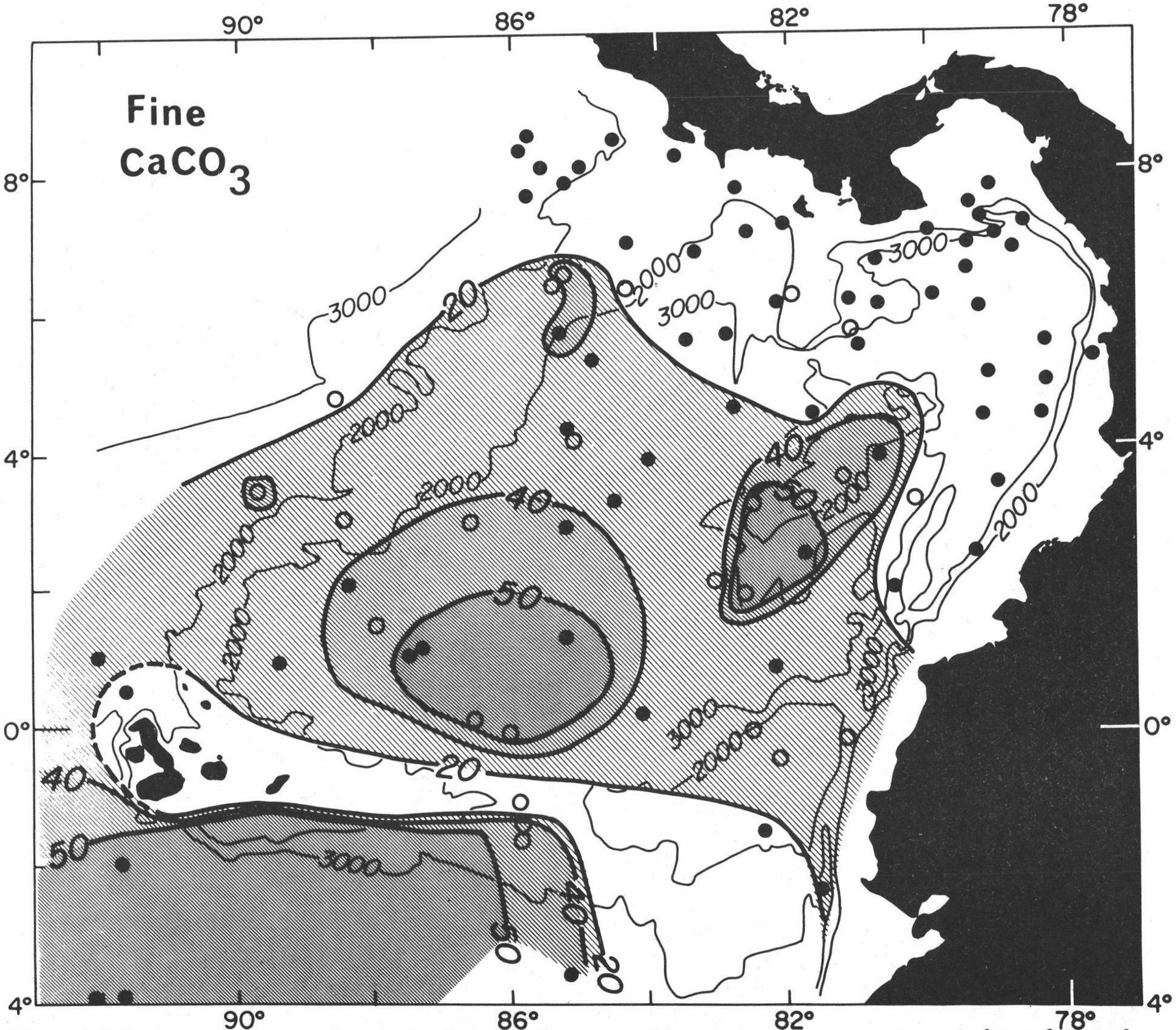

Figure 8. Distribution of fine-grain carbonate in surface sediments (percent weight of total sediment)
% Fine carbonate (weight) = % Carbonate (weight) - % Foraminifera (weight).

weight of 1 planktonic foraminifera	10 μ gm (range 1 in well pres. to 20 in poorly preserved assemblages)
weight of 1 mineral grain > 62 microns	5 μ gm
weight of 1 radiolarian skeleton (Moore, 1969)	0.05 μ gm

The weight percentage of foraminifera in the coarse fraction of each sample can be converted to weight percentage of the total sediment, since the proportion of each sample coarser than 62μ is known.

Figure 8 shows high concentrations of fine carbonate north and south of the Carnegie Ridge. The distribution is similar to that of radiolarian skeletons that have been winnowed from the ridge (Figure 4). The Malpelo Ridge, where foraminiferal fragments are abundant in the coarse fraction, is also rich in fine carbonate which may have formed by comminution of the calcareous tests. The Cocos Ridge is generally richer in fine carbonate than the Carnegie Ridge, suggesting that current action over the former is less pronounced. The region rich in fine carbonate on the crest of the north central Cocos Ridge, like that on the Malpelo Ridge, coincides with an area rich in foraminiferal pieces.

A comparison of the distribution pattern of fine carbonate (Figure 8) with the maps of fine grain-size modes of van Andel (1973, in press), shows that van Andel's modes D and E combined correlate best with the carbonate. Oser (1972) found that a mode between

6.30 ϕ and 7.90 ϕ (12.7 μ - 4.2 μ) in pelagic sediments from the North Pacific consists of pure Coccolithus pelagicus. This size range corresponds to van Andel's mode D, which ranges from 6.80 ϕ to 7.60 ϕ. This is one of the largest coccolith "species," however, and most of the coccoliths will occur in finer modes, such as van Andel's E (7.68 ϕ and 8.30 ϕ). Clearly, a detailed examination of fine carbonate particles by both electron and optical microscopy is needed to throw further light on these sediments, but it seems likely that much of the fine carbonate in the vicinity of the Carnegie Ridge consists of coccoliths.

g) Distribution of Volcanic Glass Shards

As can be seen in Figure 9, colorless glass shards are concentrated in a lobe extending from the continental margin on to the eastern Carnegie Ridge, and on the central Cocos Ridge. Smaller concentrations are found along the coasts of Colombia and Costa Rica near the Cocos Ridge. In contrast, brown shards are concentrated west of the Galapagos Archipelago, with only a single sample in the basin, between the Malpelo and the Coiba Ridges, also containing some of this type of glass.

The brown glass differs from the colorless in its larger grain size, color, blocky appearance, abundance of well formed vesicles and anisotropic mineral inclusions. Heiken (1972) terms such shards

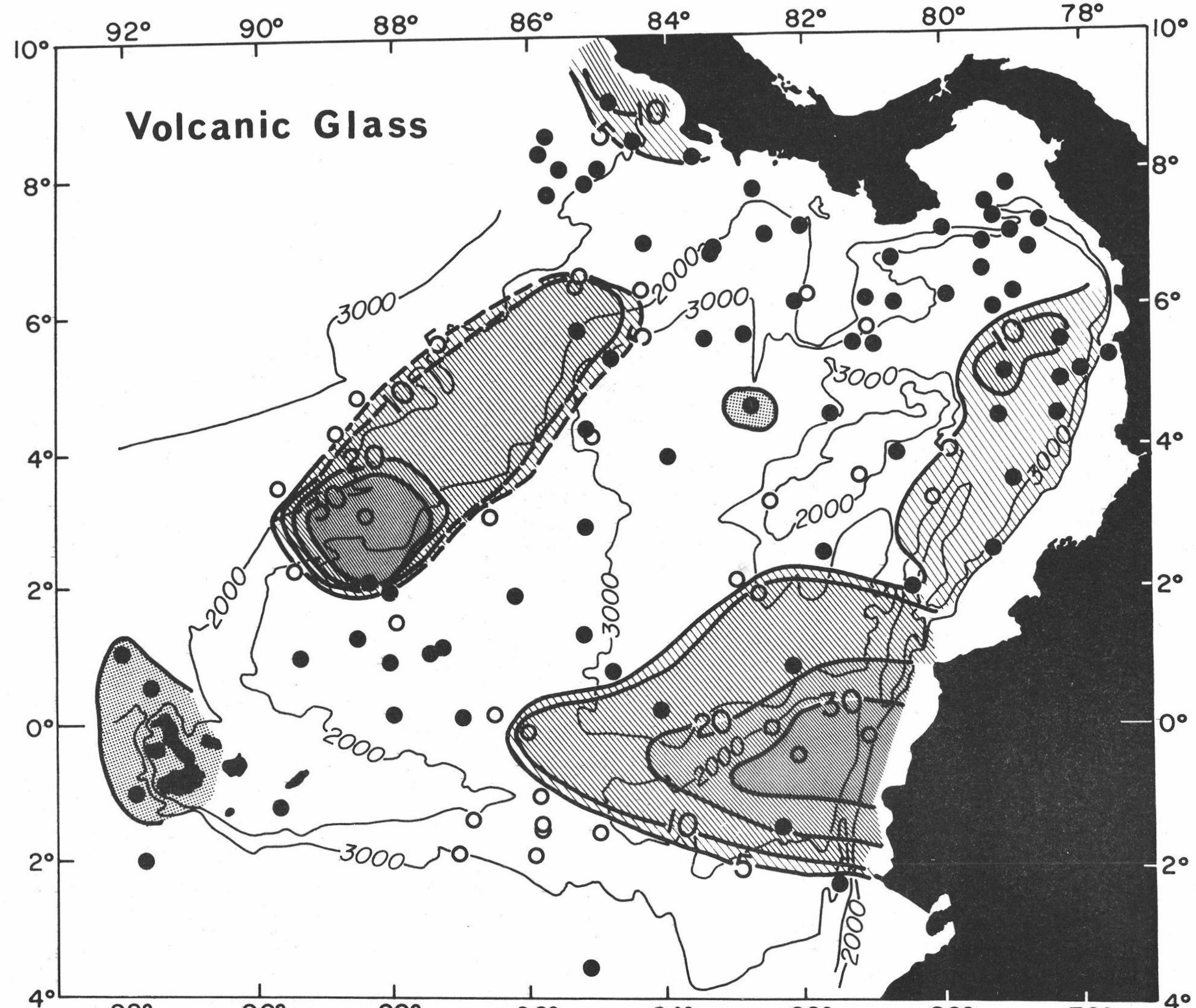

Figure 9. Distribution of colorless volcanic glass shards in surface sediments (carbonate-free coarse fraction). Dotted shading marks the area of concentration of brown glass shards.

"phraetomagmatic." They form from glasses that were rapidly quenched by contact with shallow bodies of water or ground water. Such quenching causes the glass to shatter along smooth planes, preserving the gas bubbles originally present in the magma. Since the brown glasses observed near the Galapagos are fairly rich in vesicles, one can assume that they were derived from extremely shallow marine vents or subaerial eruptions where the lava entered the ocean while still in a semi-molten state.

Shards were mounted using the technique described by Nayudu (1962) and their refractive indices determined with standard immersion oils. Brown shards making up 49 percent of the coarse fraction of sample 175, collected immediately northwest of Abermarle Island, have refractive indices ranging from 1.596 to 1.602. On the basis of curves that relate the refractive index of volcanic glass to its silica content (George, 1924, in Williams et al., 1955), this glass contains about 48% silica, that is, it is basaltic.

The colorless shards can be divided into two types. One is very clear with walls formed of bubble surfaces. The other contains striations due to stretched vesicles, and has abundant inclusions of opaque minerals. Both shard types fall into the "magmatic" category of Heiken (1972), where "magmatic" indicates explosive expansion of the gases contained in the vesicles. Such a process creates both Y-shaped shards in which three bubbles are connected by thin walls (first group) and rod shaped shards where gas bubbles become stretched (second group). Thus, all the white shards were formed by explosive subaerial eruptions.

The refractive indices of colorless shards from sample 161 on the central Cocos Ridge range from 1.500 to 1.504, whereas shards with stretched bubbles from sample 192 near the Carnegie Ridge have refractive indices ranging from 1.502 to 1.506. The silica content of both types of colorless shards is, therefore, about 70% SiO_2. Explosive eruptions are most commonly associated with viscuous acidic magmas, thus both the composition of the source magma and the shard morphology agree with an explosive mode of eruption.

The transparent colorless shards are found on the north and central Cocos areas, whereas the shards with stretched bubbles and opaque inclusions occur along the coast of Colombia and on the Carnegie Ridge. Both occurrences are close to regions of intense Quaternary volcanism. Gansser (1950) mentions that andesitic and dacitic volcanism occur in southern Colombia west of the Central Cordillera, at the same latitude as the Carnegie Ridge glass-rich samples. Quaternary volcanoes occur west of Puntarenas, Costa Rica (Lloyd, 1963; King, 1969), again at the latitude of the Cocos Ridge glass-rich deposits offshore. Most of the volcanoes here are andesitic and basaltic, but local fumaroles are rhyolitic and dacitic (Weyl, 1961). The Panama area is devoid of Quaternary volcanoes, probably because oceanic crust is not presently being subducted beneath Panama (van Andel et al., 1971a; Malfait and Dinkelman, 1972), and no glass shards are found offshore.

It is apparently surprising that most of the volcanic activity is andesitic in character, but the glass shards studied are clearly acidic. The answer must lie in the character of the eruptions producing the shards. As already mentioned, the transparent shards show signs of explosive eruption. Such eruptions eject debris higher into the atmosphere than the more voluminous but less viscous outpourings of andesitic glasses. Surface winds in the Panama Basin are variable, but weak westerlies predominate (Stevenson et al., 1970). From 850 mb to 500 mb, which at Guayaquil correspond to 1500 m to 6000 m, winds become easterly, with peak velocities occurring between 700 and 500 mb (U. S. Navy, 1959; Lamb, 1970). Thus, it appears that only the colorless shards are ejected high enough to be entrained in the strongest easterlies and carried for considerable distances. The limited dispersion of basaltic shards from the non-explosive volcanic centers in the Galapagos substantiates these conclusions.

The mechanism described above does not seem to be capable of explaining the distribution of glass shards on the central Cocos Ridge. Concentrations in this area increase to the southwest, and the region of shard-rich sediments does not seem to merge with the nearshore glass deposits of the northeast Cocos Ridge. The character of the glasses, as well as their refractive indices are identical, however. Cocos Island is a possible source, but it does not lie at the center of the colorless shard occurrence, and its rocks are basic rather than acidic (McBirney and Williams, 1969). It appears that the isolated area of ash-rich sediments is a lag deposit formed by current winnowing of the ridge crest. The high concentrations of foraminiferal pieces on the flanks of the ridge, the very low content of radiolaria in the ash-rich deposits, and the extremely thin sediment cover in the area (van Andel et al., 1971a) seem to confirm this hypothesis. Although sand-sized glass shards are hydraulically equivalent to quartz grains only half their size (Fisher, 1965), they are still hydraulically large compared to radiolarian skeletons.

h) Distribution of Anisotropic Minerals (Carbonate-free)

As expected, sand-sized non-biogenic particles are concentrated on the continental margin, with highest values occurring on the shelf (Figure 10). The coarse sand at the edge of the shelf in the Gulf of Panama has been identified by Golik (1965) as being of transgressive origin. The Galapagos Archipelago also contributes coarse terrigenous material. The extremely low quartz content of these sediments (Heath et al., 1973, in press) results from the petrology of the islands; they are mainly tholeiitic basalt, olivine tholeiites and alkali-olivine basalts (McBirney and Williams, 1969).

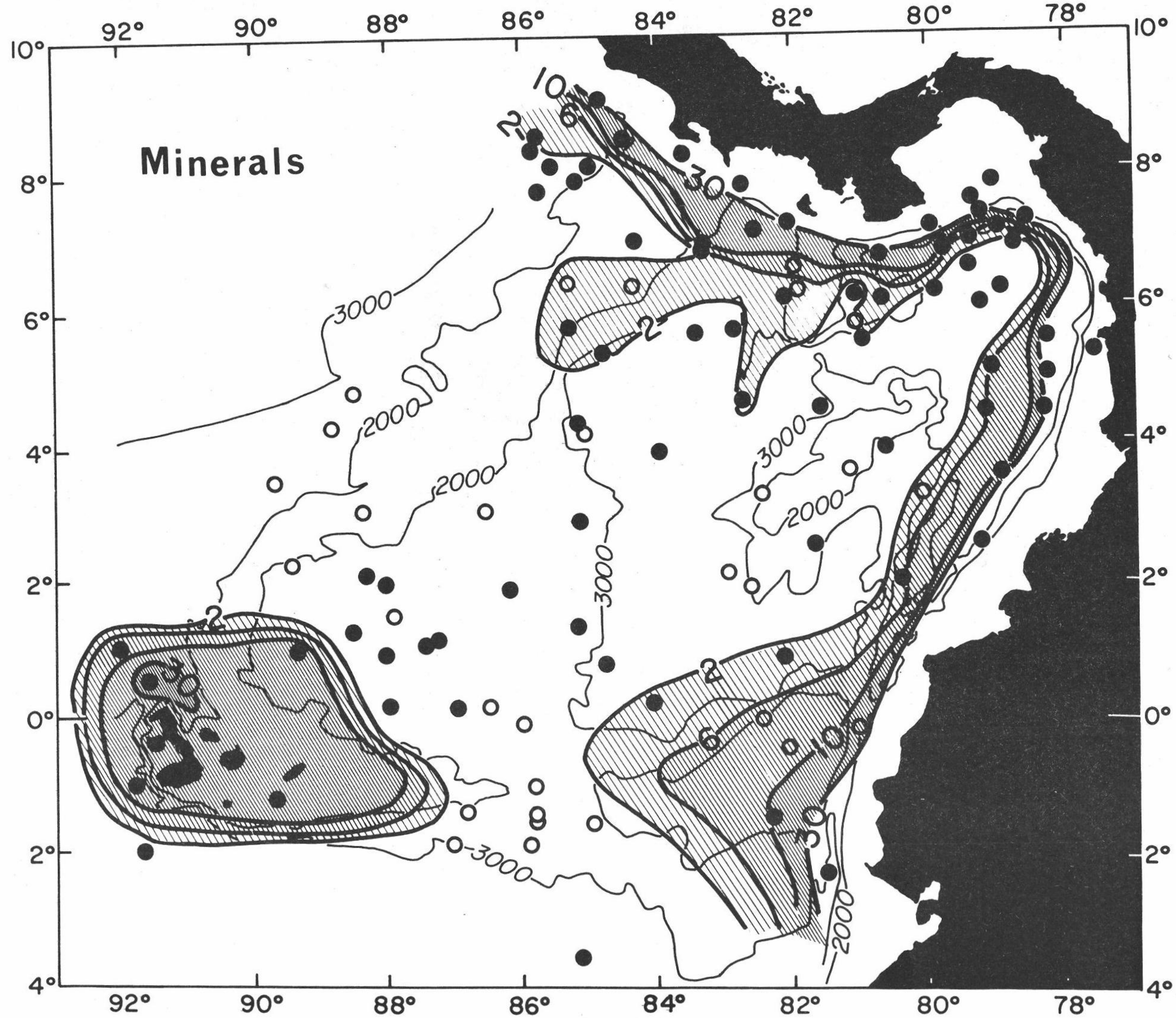

Figure 10. Distribution of anisotropic mineral grains in surface sediments (carbonate-free coarse fraction).

Two mineral-rich tongues extend from the continental margin. The northern one is terrigenous sediment that was probably transported by bottom contour currents. Silt Mode C of van Andel (1973, in press) shows the same distribution pattern. The southern tongue on top of the east Carnegie Ridge coincides with an area of abundant colorless glass shards (previous section). Since terrigenous sand cannot reach the ridge because the topographic depression between the ridge and the continental slope acts as a barrier, the sands on the Carnegie Ridge must be transported by some other agent. The co-occurrence of mineral particles and volcanic glass, together with the areal extent of these deposits suggest eolian transport. Similar lobate volcanic deposits transported by wind and including heavy minerals as well as glass shards have been reported by Lisitzin (1972, page 184), and Naboko (1947).

Only four samples from the continental margin contain enough heavy minerals to allow their separation. Two of these samples (1, 3) come from the shelf of the Panama Gulf and the other two (137, 147) were collected on the continental shelf at the northeast end of the Cocos Ridge. Microscopic inspection reveals abundant green hornblende and basaltic hornblende with common diopside and minerals of the epidote group, lesser amounts of hypersthene, and trace amounts of garnet. The two northern (Cocos) samples contain the more volcanic suite, which is rich in basaltic hornblende and hypersthene.

The frothy glass matrix surrounding each mineral grain confirms their volcanic origin. Possible sources for the Gulf shelf sands include Late Mesozoic eugeosynclinal volcanic and clastic deposits, and Quaternary coastal plain clastics (King, 1969). The large quartz-diorite pluton of the Peninsula of Azuero (Ferencic et al., 1968) probably supplies most of the green hornblende and epidote found in the Gulf shelf samples.

i) Minor Components

Glauconite. Except for an obvious increase in abundance towards shore, the occurrence of glauconite sediments is irregular. Glauconite associated with foraminiferal pieces is common in sediments at two locations on the northeast Cocos Ridge. It is also common around the Coiba Ridge, and locally on the Carnegie and southwest Cocos Ridges.

The glauconite associated with foraminiferal tests probably formed as internal molds (Ehlmann et al., 1963). The occurrence along the continental shelf, like many similar occurrences (Emery, 1968), are associated with the basal transgressive sands deposited during the Holocene rise in sea level.

Benthic Foraminifera. Ratios of benthic to planktonic foraminifera have been used as depth indicators (for example, Stehli and

Creach, 1964). Although Funnell (1967) did not believe that depth is the controlling variable, he observed that benthics are more abundant on continental shelves, and are inversely correlated with the abundance of planktonics. This cannot be confirmed here since the sampling on the continental shelf is very sparse.

Parker and Berger (1971) noted that in the deep sea, the planktonic to benthic ratio is primarily a function of preservation. In well-preserved assemblages the ratio is high while in badly preserved ones, it is low. This is well demonstrated in the Panama Basin. Benthic foraminifera are present (although in small absolute numbers) in the areas where carbonate dissolution is most pronounced, such as the north Cocos, Malpelo and Coiba Ridges. These areas are rich in fragments of planktonic foraminifera.

Diatoms. Because the samples analyzed in this study were sieved through a 62μ mesh, most of the diatom population was not retained. Diatoms generally range from 10 to 100 μ in diameter (Riedel, 1963), in contrast to radiolaria which generally range from 50 to 400 μ in diameter and are, therefore, the dominant form of opaline silica in the coarse fraction (Riley and Chester, 1971).

The highest concentration of diatoms observed in the coarse fraction is less than 1% (sample 57 west of the Coiba Gap). All specimens are badly preserved. Frustules are discoidal

(Coccinodiscus) and approximately 100 microns in diameter.

Sponge Spicules. Spicules make up a significant portion of the carbonate-free coarse fraction only in one sample from the Galapagos Platform (27%) and another immediately north of it (17%). Everywhere else, their abundance is 1% or less, and does not vary systematically over the basin.

Sponges are benthic animals that live attached to the bottom. Therefore, they need a solid substratum. Because of their fragile structure, they prefer low energy environments. As filter feeders, they thrive in somewhat agitated waters rich in organic debris but low in terrigenous material. Optimum growth conditions require well oxygenated and nutrient-rich waters (Meglitsch, 1967).

Apparently, depth is not a decisive factor, because sponges are found from the shallowest depths to the abyssal sea floor (Moore, 1958). Sokolova (1959) related the location of benthic communities to topography, and indirectly to sediment accumulation rates. Sponges as well as other filter feeders occur where sedimentation rates are low. Thus, they prefer the edge of the continental shelf or even better, the edge of submarine banks where basement outcrops can serve as "footholds." Sample 64 is at the edge of the Galapagos Platform. Water circulation is quite active, judging by the coarse foraminiferal sand and the badly preserved radiolaria present in the sample. In fact, the large sponge spicules are probably concentrated with the coarsest components by current winnowing.

Almost all types of spicules are represented in the Galapagos samples: monoaxons (curved, monoactinic and diactinic), thorny rhabds, hexactinic and triradiate spicules and sphaeraster. In other samples, amphidiscs are also present.

DEPTH DISTRIBUTION OF CARBONATE COMPONENTS

Moore _et_ _al_. (1973, in press) have established that the calcite compensation depth (CCD) in the Panama Basin is about 3400 m. This is much shallower than the 4500 m and 4700 m depths found in the south and central equatorial Pacific, respectively. If the proportions of whole foraminifera and foraminiferal fragments are plotted against depth (Figure 11), it is apparent that the foraminiferal compensation depth, like the CCD, lies at 3400 m.

In Figure 12, whole foraminifera and fragments are distinguished. Both are expressed as percentages of biogenic components only so as to minimize the effects of terrigenous dilution. The dotted line is the envelope enclosing all samples containing whole foraminifera. Its deepest limit is the "whole foraminifera" compensation depth, and has a value of 3400 m, the same as the CCD. Within the envelope, most of the samples rich in whole foraminifera are found near 2200 m. This peak is readily explained by the physiography of the basin.

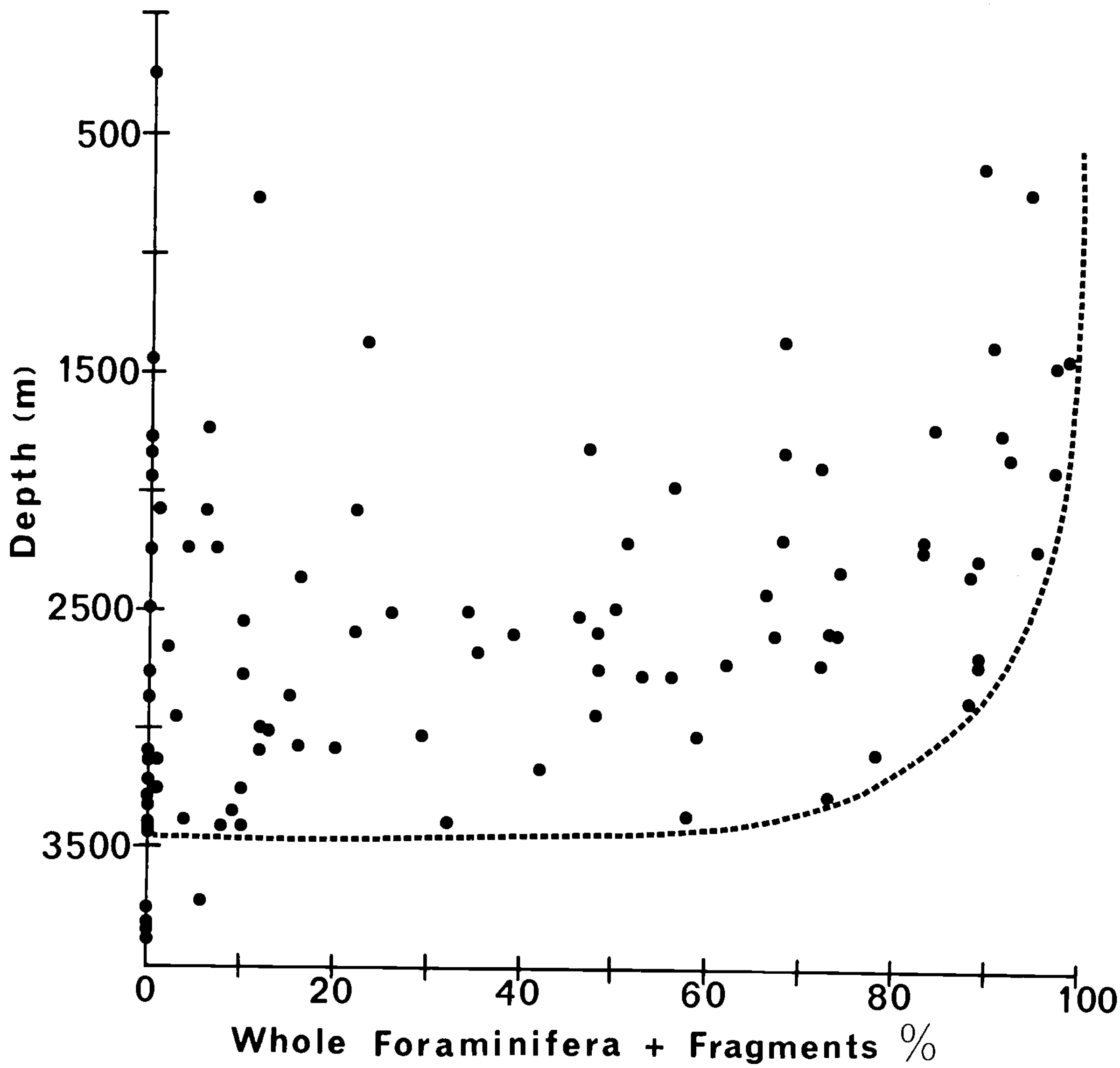

Figure 11. Abundance of planktonic foraminifera vs. depth. Horizontal portion of the dotted line is the foraminiferal compensation depth. Abundance of foraminifera in % of coarse fraction.

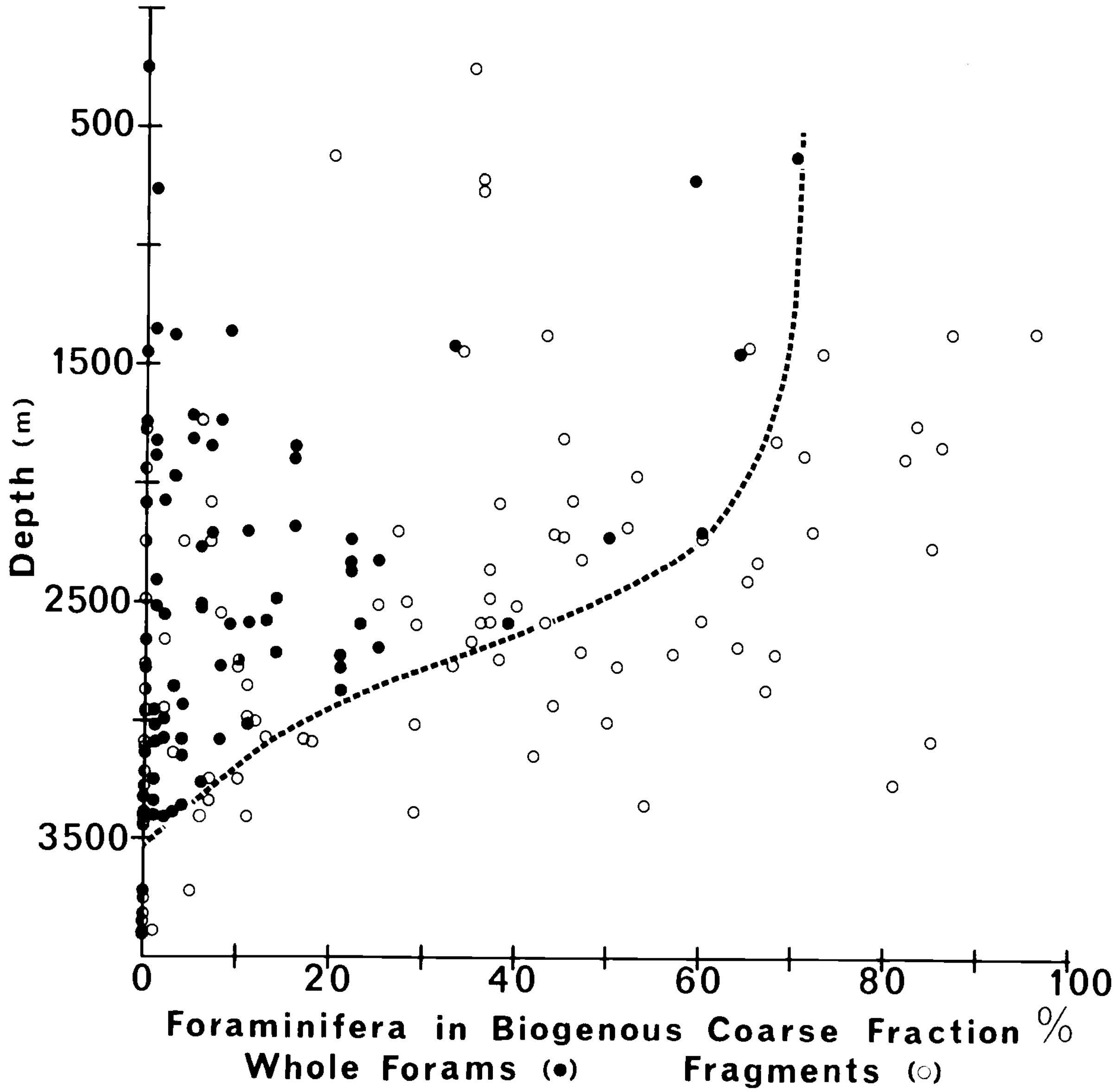

Figure 12. Abundance of whole planktonic foraminifera and fragments vs. depth. Base of the dotted line marks the compensation depth for whole foraminifera.

The 2200 m contour outlines the ridges on which whole foraminifera are ubiquitous. The low values in the 2200 m depth range belong to samples from several locations, including the anomalous northeastern Cocos Ridge and the Malpelo Ridge.

The foraminiferal fragments (open circles in Figure 12) show a different distribution. Below 1500 m, they are very abundant but there is a considerable scatter of the points. The rapid increase in fragments at 1500 m, may well be a result of severe carbonate dissolution (discussed below). The scatter of the data below 1500 m, shows little relationship with depth, and reflects the heterogeneity of the basin, and the importance of reworking and redeposition as well as dissolution on the distribution of calcite grains.

If the non-carbonate portion of the sediment is assumed constant, it is possible to estimate the proportion of carbonate dissolved as a function of water depth. Figure 13 shows the results of such calculations for terrigenous-free calcium carbonate (data from Moore _et al._, 1973, in press) and for whole foraminifera (whole forams + radiolaria = 100%). Dissolution values are averaged over 500 m depth intervals and plotted at the middle of each interval. For the shallowest interval, in which samples are rare, data were averaged from 617 - 1500 m. For the total carbonate, a non-carbonate concentration of 5% was assumed in undissolved sediment. A value of 7% was used for the whole foraminifera. These values were based on the

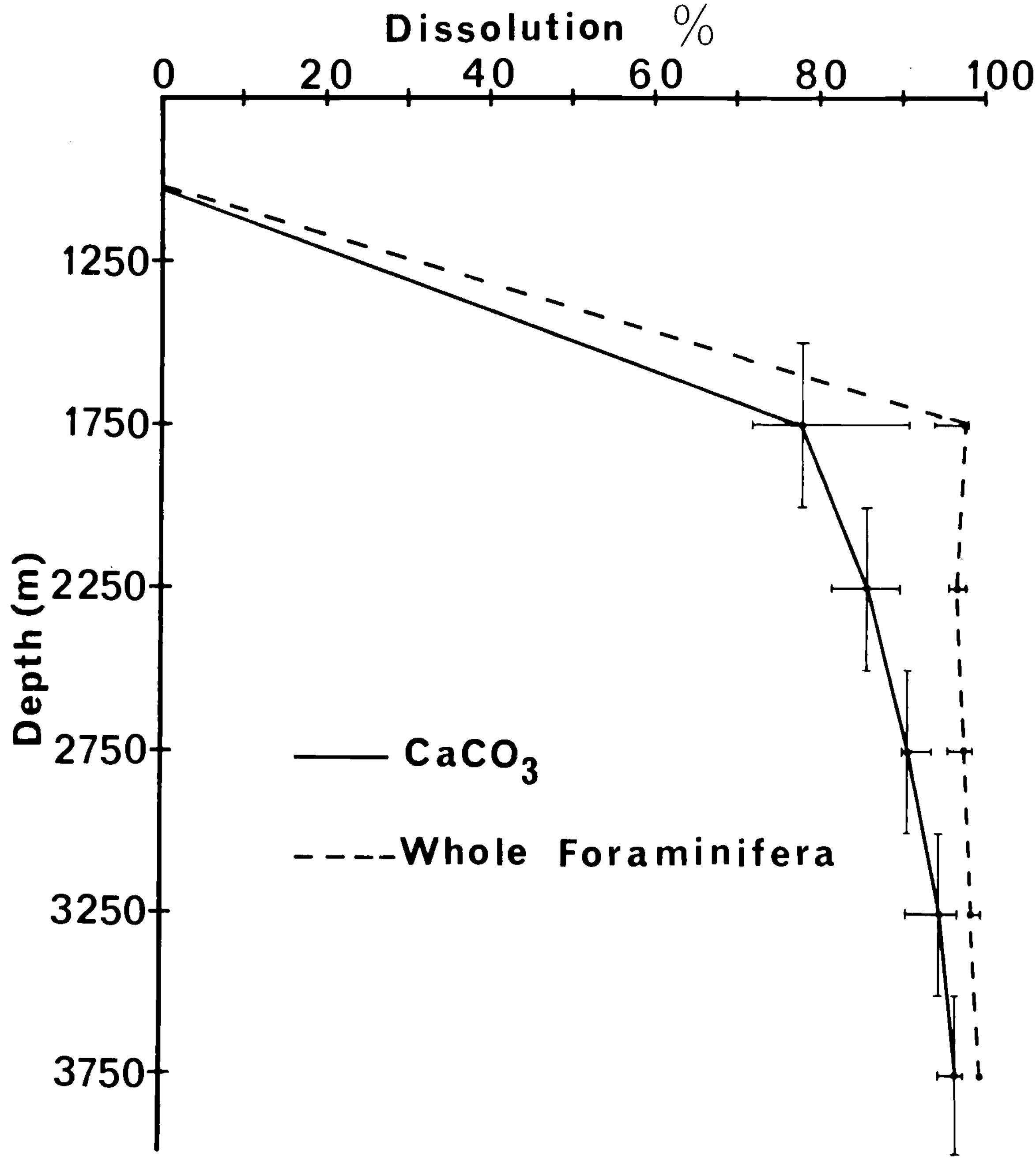

Figure 13. Percent dissolution of calcium carbonate and whole foraminifera as a function of depth, assuming initial concentrations of 5% and 7% non-carbonate, respectively. Median values of carbonate and whole foraminifera contents (terrigenous-free) at 500 m depth intervals were used to calculate the amount of dissolution. Horizontal bars show values of dissolution calculated using the 80% confidence limits for the medians of the concentrations of carbonate and whole foraminifera. Vertical bars, equal for both carbonate and foraminifera, show the depth intervals over which the median concentrations were calculated.

least dissolved samples in the suite, and are undoubtedly conservative. The medians of the carbonate and foraminiferal percentages for each depth interval were used in the calculations of dissolution, because the data are not normally distributed. Samples from the continental shelf that lacked planktonic foraminifera due to dilution have been excluded from the calculations.

Horizontal bars through the dissolution values of Figure 13 are the 80% range "confidence limits" for the medians (Tate and Clelland, 1957, Table D). Vertical bars indicate the depth intervals for which each dissolution value was calculated.

The most striking feature of both curves is the degree of dissolution at shallow depths. By 1500 m, 80% of the carbonate has dissolved and 98% of the whole foraminifera have either been fragmented or completely dissolved. These calculations are consistant with Berger's (1971) observations that "well preserved" foraminiferal assemblages in the South Pacific have already lost 50% of the fauna due to dissolution. The toll must be even greater in the Panama Basin, where oxidation of organic matter beneath the productive upwelling surface waters produces unusually corrosive bottom water.

VECTOR ANALYSIS

As an objective check on the results and conclusions of Section II, the coarse fraction data were analyzed by the vector analysis technique of Imbrie and van Andel (1964). Vector analysis is essentially a principal component analysis. It differs from the standard factor analysis in that it describes samples in terms of end-members of the total suite (Q-Mode). The number of end-members (number of factors) is specified by the user of the computer program. This technique reduces a large number of variables to a comprehensible and mappable set of extreme factors.

A three factor system, which accounted for 95% of the variability among the Panama Basin samples, gave the end-members shown in Table I. Depth is expressed as percentage of range. Temperature is expressed as percentage of range of the natural logarithm of the bottom potential temperature at each sample location. The logarithm is used to stress horizontal temperature differences due to the migration of cold water masses and to minimize the influence of depth on the temperature of the water column. The varimax loading for the first, second and third factors are 46%, 33% and 20%, respectively. This indicates that none of the factors represents a trace component.

The first end-member (sample 142) primarily represents samples rich in radiolaria and opal, but low in $>62\mu$ particles, that are found in deep and cold water. The distribution of this vector in the basin is shown in Figure 14. High values are found in the eastern basin where siliceous material is abundant and where continental

Table 1. End Members (three factor vector analysis)

	Factor 1 Sample 142	Factor 2 Sample 17	Factor 3 Sample 137
Depth	78.9%	29.4%	40.1%
Radiolaria (carbonate-free)	99.2	4.2	1.2
Carbonate*	15.7	95.4	5.2
Opal (carbonate-free)*	41.2	22.9	11.2
Terrigenous	49.6	3.5	84.2
Bottom Water Temp.	8.4	35.1	20.3
>62 μ	0.7	87.0	14.0
Whole Planktonic Forams	0.0	33.4	0.0
Planktonic Foram Fragments	0.2	64.9	0.0
Minerals (>62μ, carbonate-free)	1.1	1.0	99.5
Transparent Glass	0.0	29.0	1.2
Glauconite	0.2	53.9	22.4

*from Moore et al. (1973, in press)

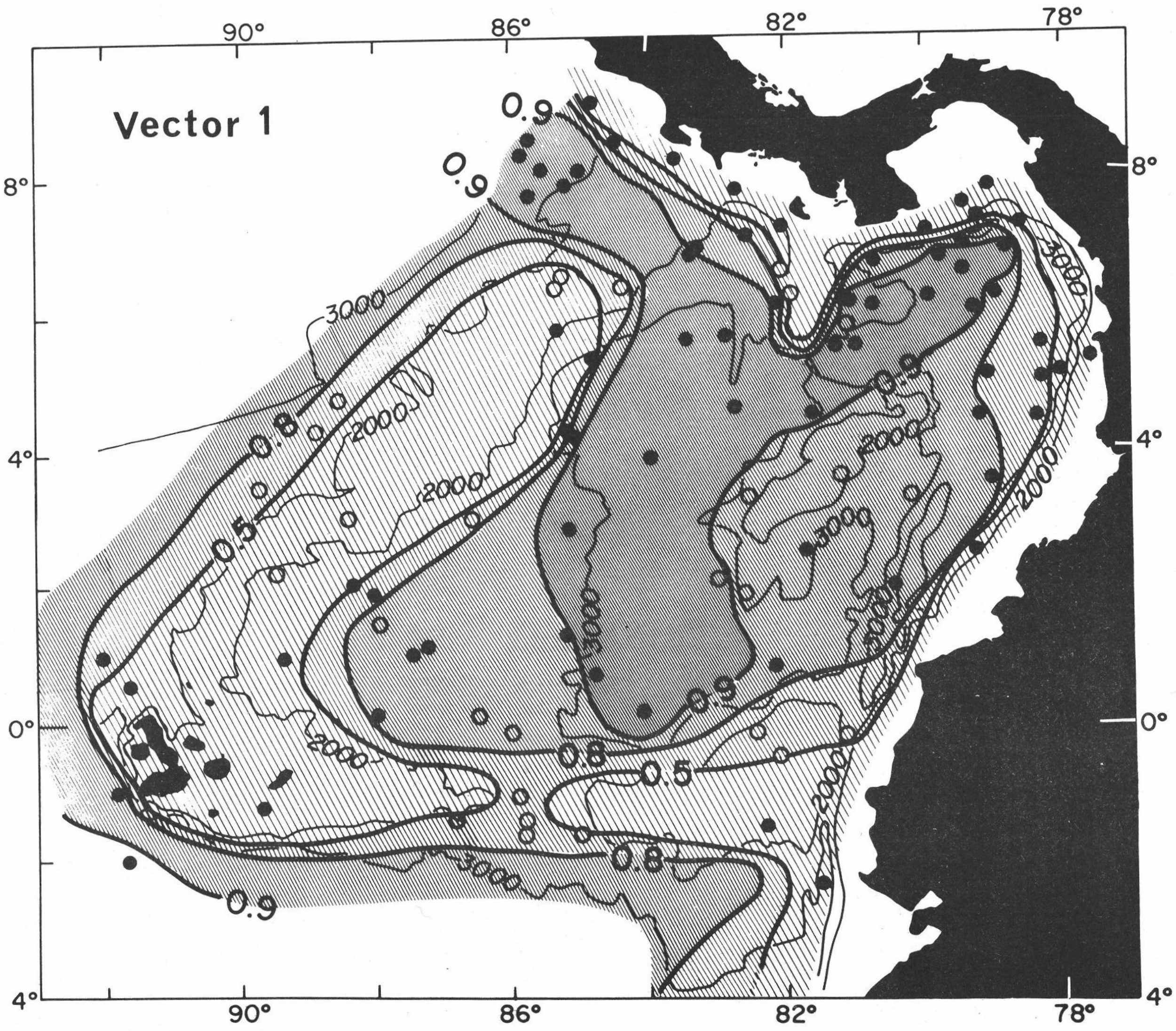

Figure 14. Contours of Q-mode vector 1 ("opaline end-member") in surface sediments of the Panama Basin.

runoff deposits terrigenous clays. Low values reflect the lack of siliceous material on the ridges. These observations substantiate the conclusions reached on the distribution of radiolaria in Chapter II.

The second end-member (sample 17) represents samples rich in calcium carbonate, foraminiferal components, and coarse ($>62\mu$) particles. Such samples are found in warm, relatively shallow water. The areal distribution of this vector is shown in Figure 15. High values are found on the isolated ridges, particularly in the western basin. These results resemble both the foraminiferal map and the carbonate map of Moore _et al_. (1973, in press) presented in Chapter II.

The third end-member (sample 137) is representative of samples rich in terrigenous material, both coarse and fine-grained. As shown in the third map (Figure 16), contours of this vector hug the continental shelf and slopes, except where a tongue of sediment extends along the southern flank of the northeast Cocos Ridge. A similar lobe can be seen in one of the grain size maps of van Andel (1973, in press). The general pattern is similar to that of the mineral map presented in Chapter II as well as to the map of quartz abundance (Heath _et al_., 1973, in press), but is not influenced by the volcanic components of the sediment. Neither the concentrations of colorless glass on the central Cocos Ridge nor the glass-rich sediments on the eastern Carnegie Ridge appear in the vector map. The

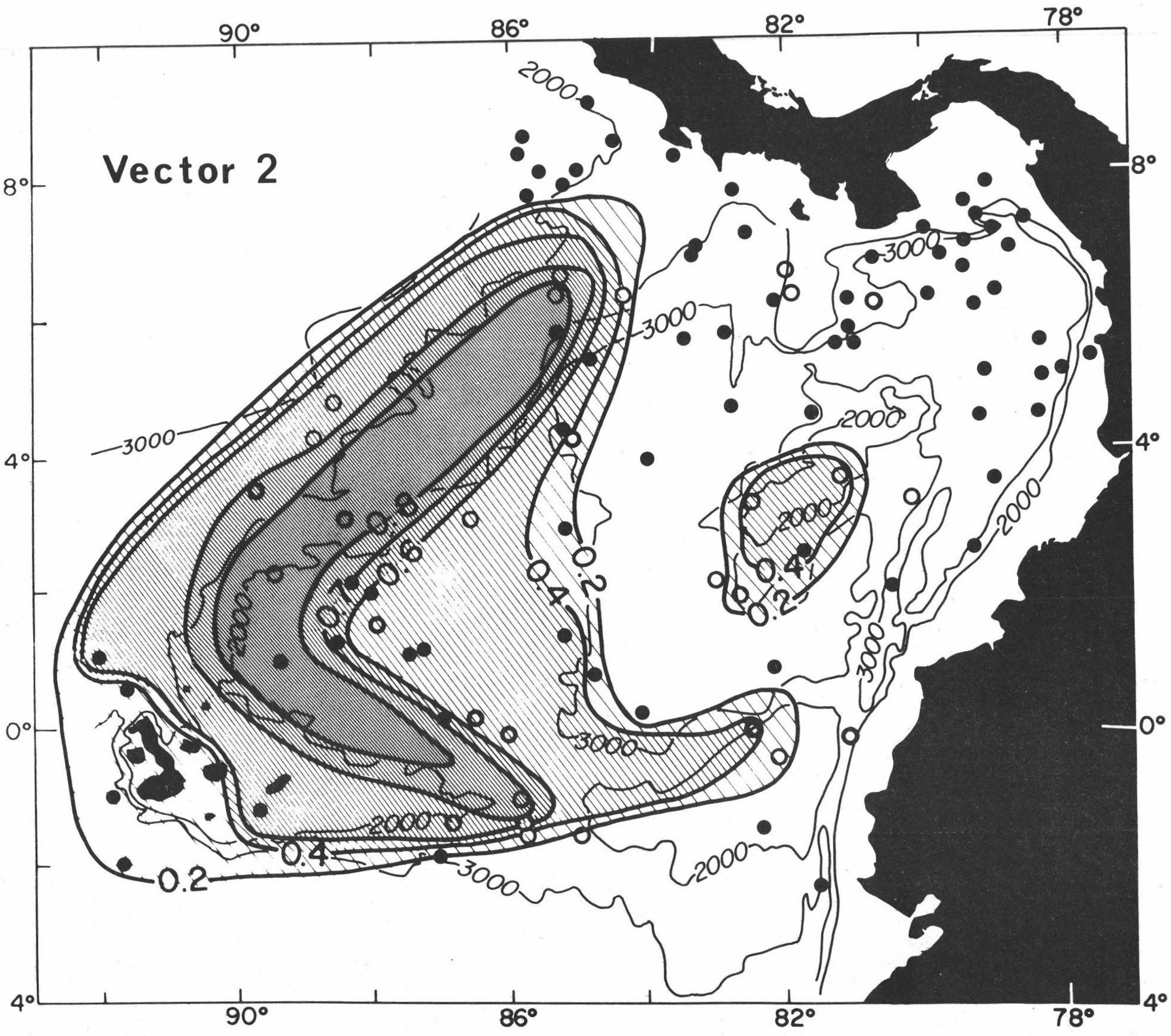

Figure 15. Contours of Q-mode vector 2 ("carbonate end-member") in surface sediments of the Panama Basin.

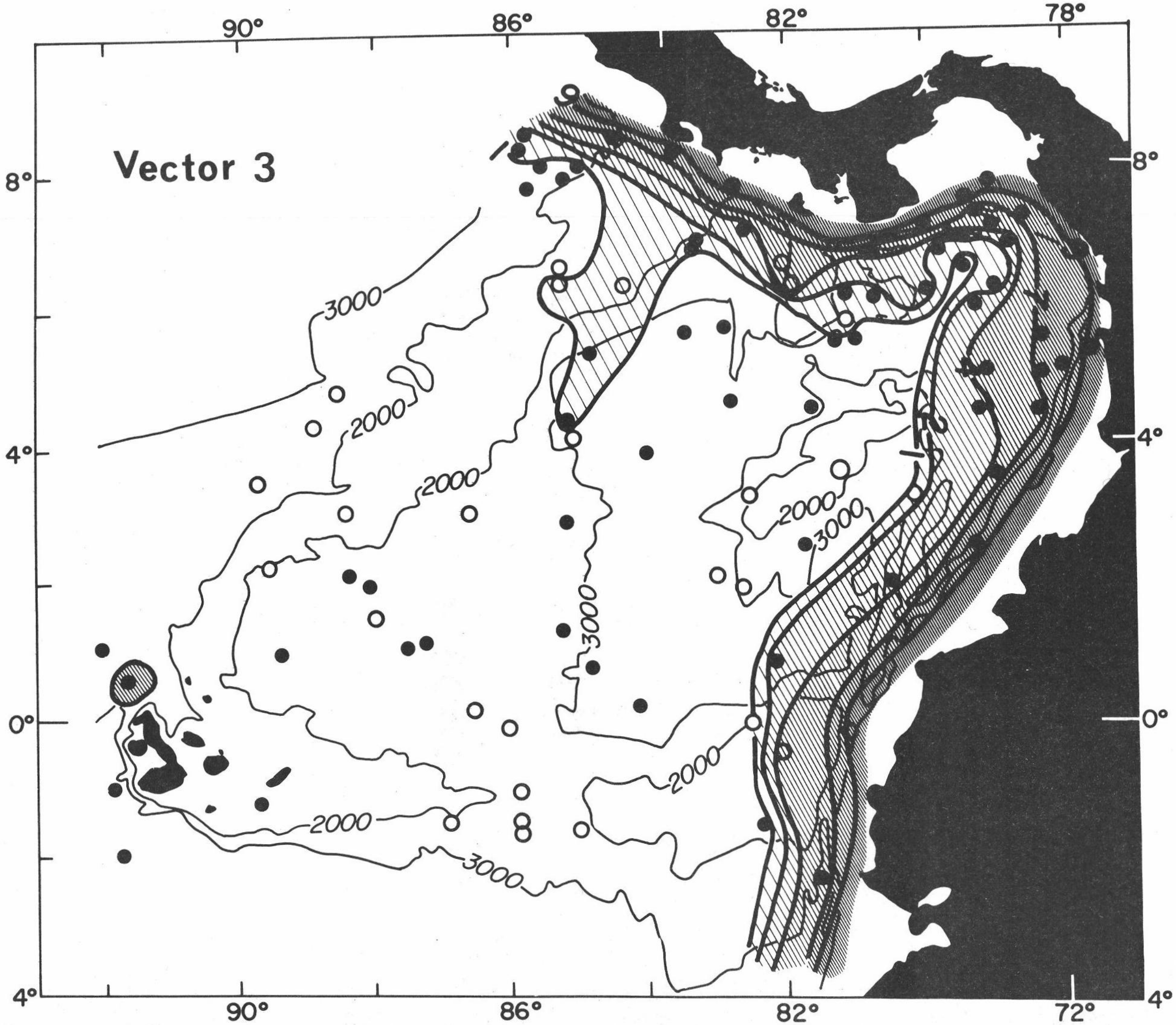

Figure 16. Contours of Q-mode vector 3 ("terrigenous end-member") in surface sediments of the Panama Basin.

brown glass off the Galapagos Islands is reflected in this vector, however.

Vector analysis using five end-members produced patterns even more similar to those of Chapter II. The first two factors are geologically redundant and group radiolaria and terrigenous clay in one case, and radiolaria and opal at great depths in the other. The third factor is identical to the third factor in the three component system, with the addition of glauconite. This is the glauconite associated with the relict sands at the shelf edge in the Panama Gulf. The fourth and fifth factors split the carbonate components into foraminiferal pieces (associated with glauconite and volcanic glass shards) and whole foraminifera respectively.

SUMMARY

The coarse sediments in the Panama Basin reflect an environment dominated by current action. Winnowing of ridge sediments help break foraminiferal shells, it exposes them to dissolution by bottom waters and, it removes the skeletons of radiolaria, depositing them in the deeper parts of the basin. Indirect evidence indicates that fine-grained carbonate, probably coccoliths, is also being redeposited in the inter-ridge basin. Coarse foraminiferal sand and volcanic glass shards are left behind on the ridge crests. Foraminiferal fragments make up an average of 50 percent of the coarse fraction of reworked samples, but only 18% of unreworked samples. Reworking overshadows the effect of increasing dissolution of carbonate sediments with depth and masks the effect of surface high primary productivity on the distribution patterns of biogenic sediments.

Areal distributions of the sediment components and of vectors incorporating all components reveal the strong influence of the topography of the basin on sedimentation. No foraminifera are found in sediments deposited below 3400 m, the calcite compensation depth for the basin. The CCD is extremely shallow compared to other equatorial regions of the Pacific because the high production of high concentrations of organic matter in the surface waters is not balanced by foraminiferal production. Organic matter is provided by coastal upwelling that leads to high biologic productivity and by continental runoff. Oxidation of the organic matter at depth increases the carbon dioxide content of the bottom waters, rendering them more corrosive to calcium carbonate. This corrosiveness results in very high relative rates of dissolution of calcium carbonate and foraminiferal tests at shallow depths. Eighty percent of the total carbonate is dissolved and 98% of the foraminifera are either dissolved or broken between 600 and 2000 meters. As a result, the eastern basin which is for the most part below the CCD, is poor in carbonate sediments. Cold bottom waters of the Panama Basin penetrate along the Peru-Chile

Trench and contribute to the dissolution of the carbonate.

Volcanic sediments, mostly colorless acidic glass shards are concentrated in tongues north and south of the basin, reflecting the distribution of Quaternary continental volcanoes and the direction of easterly winds. The shards originate from explosive eruptions characteristic of viscous magmas. Brown basaltic shards are found immediately west of the Galapagos Archipelago. They have the quenched appearance of glasses derived from shallow submarine flows or littoral eruptions.

Terrigenous sands are restricted to the edge of the continental shelf and slope. Authigenic glauconite associated with them indicates an environment of non-deposition typical of relict sands. Contour currents seem to have transported terrigenous material into the north part of the basin.

BIBLIOGRAPHY

Arrhenius, G. O. 1963. Pelagic sediments. In: The Sea, ed. by M. N. Hill. Vol. 3 New York, Interscience. p. 655-727.

Berger, W. H. 1971. Sedimentation of Planktonic Foraminifera. Mar. Geol. 11:325-358.

Bramlette, M. N. 1961. Pelagic sediments. In: Oceanography. Lectures at the International Oceanographic Congress, ed. by Mary Sears, New York, 1959. AAAS Publ. 67:345-366.

Campbell, A. S. 1954. Radiolaria. In: Treatise on Invertebrate Paleontology, ed. by R. C. Moore. University of Kansas Press and Geol. Soc. Am. (Pt. D), Protista 3, 11.

Chayes, F. 1960. On correlation between variables of constant sum. J. Geophys. Res. 65(12):4185-4193.

Cox, R. A., M. J. McCartney and F. Culkin. 1970. The specific gravity/salinity/temperature relationship in natural sea water. Deep-Sea Res. 17:679-689.

Culberson, C. H. 1972. Processes affecting the oceanic distribution of carbon dioxide. Ph. D. Thesis. Oregon State University, Corvallis. 178 numb. leaves.

Ehlmann, A. J., N. C. Hulings and E. D. Glover. 1963. Stages of glauconite formation in modern foraminiferal sediments. J. Sed. Pet. 33(1):87-96.

Ellis, D. B. 1972. Holocene sediments of the South Atlantic Ocean: the calcite compensation depth and concentration of calcite, opal and quartz. Master's Thesis. Oregon State University, Corvallis. 77 numb. leaves.

Emery, K. O. 1968. Relict sediments on continental shelves of the world. Bull. Amer. Assoc. Pet. Geol. 52:445-464.

Ferencic, A., D. del Giudico and G. Recchi. 1968. Tectomagmatic and metallogenic relationships of the central Panama-Costa Rica region. Trans. Fifth Carib. Geol. Conf., Geol. Bull. No. 5, Queens College Press, 250 p.

Fisher, R. V. 1965. Settling velocity of glass shards. Deep-Sea Res. 12:345-353.

Fofonoff, N. P. 1962. Physical properties of sea water. In: The Sea, ed. by M. N. Hill. Vol. 1 New York, Interscience, p. 3-30.

Forsbergh, E. D. 1969. On the climatology, oceanography and fisheries of the Panama Bight. Inter-American Tropical Tuna Commission. Bull. 14(2):49-385.

Funnell, B. M. 1967. Foraminifera and radiolaria as depth indicators in the marine environment. Mar. Geol. 5:333-347.

Gansser, A. 1950. Geological and petrographical notes on Gorgona Island in relation to northwestern South America. Schweitz. Miner. u. Petrogr. Mitt. Band 30, Heft 2, p. 219-237.

George, W. O. 1924. The relation of the physical properties of natural glasses to their chemical composition. J. Geol. 32(5):353-372.

Golik, A. 1965. Foraminiferal ecology and Holocene history, Gulf of Panama. Ph. D. Thesis. University of California, San Diego. 197 numb. leaves.

Haeckel, E. 1887. Report on the radiolaria collected by H. M. S. Challenger during the years 1873-76. Rep. Voyage Challenger, Zool. 18:1803 p.

Haiken, G. 1972. Morphology and petrography of volcanic ashes. Geol. Soc. Am. Bull. 83:1961-1988.

Heath, G. R., T. C. Moore and L. Dowding. 1973. Mineralogy of surface sediments: Panama Basin, eastern equatorial Pacific. (in press).

Horn, D., M. Delach and B. Horn. 1969. Distribution of volcanic ash layers and turbidites in the North Pacific. Geol. Soc. Am. Bull. 80:1715-1724.

Imbrie, J. and Tj. H. van Andel. 1964. Vector analysis of heavy mineral data. Geol. Soc. Am. Bull. 75:1131-1156.

King, P. B. 1969. Tectonic map of North America. United States Geological Survey. 1:5000000.

Laird, N. P. 1971. Panama Basin Deep Water - properties and circulation. J. Mar. Res. 29(3):226-234.

Lamb, H. H. 1970. Volcanic dust in the atmosphere with a chronology and assessment of its meteorological significance. Phil. Tran. Roy. Soc. Lond. 266:425-533.

Lisitzin, A. P. 1972. Sedimentation in the World Oceans. SEPM Special Publication No. 17, 218 p.

Lloyd, J. 1963. Tectonic history of the south Central - American Orogen. In: Backbone of the Americas, ed. by Childs and Beebe. Amer. Assoc. Pet. Geol. Memoir 2, p. 88-100.

Lonsdale, P., W. R. Normark and W. A. Newman. 1972a. Sedimentation and erosion on Horizon Guyot. Geol. Soc. Am. Bull. 83:289-316.

Lonsdale, P., B. T. Malfait and F. N. Spiess. 1972b. Abyssal sand waves on the Carnegie Ridge. Geol. Soc. Am. Abstracts 4(7):579-580.

Malfait, B. T. and M. G. Dinkelman. 1972. Circum-Caribbean tectonic and igneous activity and the evolution of the Caribbean Plate. Geol. Soc. Am. Bull. 83:251-272.

McBirney, A. R. and H. Williams. 1969. Geology and petrology of the Galapagos Islands. Geol. Soc. Am. Memoir 118, 197 p.

Meglitsch, P. A. 1967. Invertebrate Zoology. Oxford University Press, New York. 961 p.

Moore, H. B. 1958. Marine ecology. John Wiley and Sons, Inc. New York. 491 p.

Moore, T. C. 1969. Radiolaria: change in skeletal weight and resistance to solution. Geol. Soc. Am. Bull. 80(10):2103-2107.

Moore, T. C., Jr., G. R. Heath and R. O. Kowsmann. 1973. Biogenic sedimentation in the Panama Basin. (in press)

Naboko, S. I. 1947. Products of the Klyuchevskoy Volcano eruption in 1937-1938 (In Russian): Trans. Vol. Lab. and Kamchatka Volc. Sta., Issue 4.

Nayudu, Y. 1962. Rapid method for studying silt-size sediments and heavy minerals by liquid immersion. J. Sed. Pet. 32(2):326-333.

Ninkovich, D., B. Heezen, J. Conolly and L. Burckle. 1964. South Sandwich tephra in deep-sea sediments. Deep-Sea Res. 11:605-619.

Oser, R. K. 1972. Sedimentary components of Northwest Pacific pelagic sediments. J. Sed. Pet. 42(2):461-467.

Parker, F. L. and W. H. Berger. 1971. Faunal and solution patterns of planktonic foraminifera in surface sediments of the South Pacific. Deep-Sea Res. 18:73-107.

Riedel, W. R. 1963. The preserved record: paleontology of pelagic sediments. In: The Sea, ed. by M. N. Hill. Vol. 3 New York, Interscience. p. 866-882.

Riley, J. P. and R. Chester. 1971. Introduction to Marine Chemistry. Academic Press, London. 465 p.

Sokolova, M. N. 1959. On the distribution of deep-water bottom animals in relationship to their feeding habits and the character of sedimentation. Deep-Sea Res. 6:1-4.

Stehli, F. G. and W. B. Creach. 1964. Foraminiferal ratios and regional environments. Bull. Am. Assoc. Petrol. Geol. 48:1810-1827.

Stevenson, M. 1970. Circulation in the Panama Bight. J. Geophys. Res. 75(3):659-672.

Stevenson, M. R., O. G. Guillen and J. Santoro. 1970. Marine atlas of the Pacific coastal waters of South America. University of California Press, Berkeley.

Tate, M. W. and R. C. Clelland. 1957. Non-parametric and short circuit statistics. Interstate Printers and Publishers, Inc. Danville, Ill. 171 p.

Tickell, F. G. 1965. The techniques of sedimentary mineralogy. Elsevier Publishing Co., Amsterdam. 220 p.

U. S. Navy. 1959. Marine climatic atlas of the World. Vol. V. South Pacific Ocean.

van Andel, Tj. H. 1973. Texture and dispersal of sediments in the Panama Basin. (in press)

van Andel, Tj. H., G. R. Heath, B. T. Malfait, D. F. Heinrichs and J. I. Ewing. 1971a. Tectonics of the Panama Basin, eastern equatorial Pacific. Geol. Soc. Am. Bull. 82:1489-1508.

van Andel, Tj. H. and Scientific Staff. 1971b. Deep Sea Drilling Project, Leg 16. Geotimes. June 1971. p. 12-14.

Weyl, R. 1961. Die Geologie Mittelamerikas. Gebr. Borntraeger, Berlin. 226 p.

Williams, H., F. Turner and C. Gilbert. 1955. Petrography, an introduction to the study of rocks in thin sections. W. H. Freeman and Co., San Francisco. 405 p.

Wooster, W. S. and T. Cromwell. 1958. An oceanographic description of the eastern tropical Pacific. Bull. Scripps Inst. Oceanog. 7(3):169-282.

Wyrtki, K. 1965. Surface currents of the eastern tropical Pacific Ocean. Bull. Inter-American Tropical Tuna Commission. 9(5):271-304.

APPENDICES

APPENDIX I. Surface Sample

PL: Lamont PS: Scripps PO: OSU

Core	% wt. > 62 μ	Water Depth (corr. meters)	Sampler	Sample Top (cm)	Sample Bottom (cm)	Lat. (deg. min.)	Long. (deg. min.)	Samples
V15-11	15.3	249	PC	10	13	07.45	079.03	PL00001 1
V15-12	27.3	1445	PC	14	17	07.29	079.21	PL00003 3
V15-13	1.1	3116	PC	11	14	05.00	079.04	PL00005 5
V15-14	.2	3755	PC	21	24	04.25	078.20	PL00007 2
V15-15	.9	2659	PC	17	20	06.03	081.03	PL00009 4
V15-16	2.3	2266	PC	22	25	06.53	083.16	PL00011 1
V15-29	46.5	1689	PC	11	14	06.21	085.17	PL00013 3
V15-30	4.3	3266	PC	10	13	04.15	085.06	PL00015 5
V15-31	87.0	1417	PC	20	23	-01.30	082.19	PL00017 2
V17-40	.6	3091	PC	13	17	06.08	079.54	PL00019 4
V17-41	.4	3437	PC	13	16	05.58	079.15	PL00021 1
V17-42	19.0	1814	PC	13	16	03.32	081.11	PL00023 3
V17-43	5.2	3147	PC	14	17	01.52	082.37	PL00025 5
V17-44	9.5	3358	PC	15	18	-03.34	085.07	PL00027 2
V18-350	32.3	1838	PC	8	10	05.42	085.16	PL00029 4
V18-351	2.1	3007	PC	5	8	05.18	084.45	PL00031 1
V18-352	1.4	3072	PC	17	20	05.34	083.25	PL00033 3
V18-353	.5	3016	PC	8	11	06.06	082.05	PL00035 5
V18-354	59.7	1348	PC	10	13	06.12	081.54	PL00037 2
V18-355	.3	3387	PC	25	28	06.42	080.42	PL00039 4
V19-22	.5	3341	PC	14	17	07.04	078.59	PL00041 1
V19-23	1.1	3819	PC	10	13	04.56	078.16	PL00043 3
V19-24	53.5	1712	PC	9	12	03.12	080.08	PL00045 5
V19-25	12.1	2404	PC	10	13	02.28	081.42	PL00047 2
V19-27	9.1	1373	PC	10	13	-00.28	082.04	PL00049 4
V20-14	.2	3131	PC	9	12	06.04	080.39	PL00051 1
V20-15	.3	1736	PC	26	28	06.57	084.17	PL00053 3
V21-25	62.0	1359	PC	15	18	05.43	081.03	PL00055 5
V21-26	2.8	3081	PC	19	22	04.36	082.44	PL00057 2
V21-28	15.1	2714	PC	11	14	01.05	087.17	PL00060 5
V21-29	44.3	712	PC	12	14	00.57	089.21	PL00062 2
V21-30	21.4	617	PC	10	13	-01.13	089.41	PL00064 4
V21-211	71.6	1443	PC	7	10	03.00	088.23	PL00066 1
V21-212	2.5	3338	PC	9	12	02.50	085.08	PL00068 3
V21-213	9.2	1966	PC	11	14	03.11	082.25	PL00070 5
V21-214	6.9	2246	PC	13	16	03.50	080.38	PL00072 2
V21-215	.6	3418	PC	12	15	04.24	079.10	PL00074 4
V21-216	.4	761	PC	20	23	05.15	077.36	PL00076 1
V21-217	.2	1774	PC	13	16	06.11	078.57	PL00078 3
V21-218	.2	2763	PC	12	15	07.15	078.34	PL00080 5
V21-219	.3	3277	PC	12	15	06.55	079.24	PL00082 2
V24-35	.8	2869	PC	10	13	07.06	079.58	PL00084 4
V24-36	9.2	1878	PC	0	3	06.30	085.13	PL00086 1
RC8-102	29.0	2180	PC	7	10	-01.25	086.51	PL00088 3
RC8-103	9.1	2937	PC	17	20	01.16	085.10	PL00090 5
RC9-62	.4	3250	PC	17	20	06.50	078.44	PL00092 2
RC9-64	.6	3135	PC	16	19	05.30	078.18	PL00095 5
RC9-65	4.5	2074	PC	21	24	02.31	079.15	PL00097 2
RC9-66	.4	4218	PC	21	24	01.58	080.27	PL00099 4
RC9-67	2.4	3091	PC	15	18	00.49	082.09	PL00101 1
RC10-52	1.0	2243	PC	18	22	03.52	083.56	PL00105 5
RC10-250	12.1	1734	PC	0	3	06.17	084.19	PL00107 2
RC10-252	.5	3398	PC	10	13	05.28	080.58	PL00110 5
RC10-253	.4	3219	PC	45	49	06.31	079.24	PL00112 2
RC10-254	.2	3323	PC	14	17	07.17	079.14	PL00114 4

APPENDIX I. Surface Samples

Core	% wt. > 62 μ	Water Depth (corr. meters)	Sampler	Sample Top (cm)	Sample Bottom (cm)	Lat. (deg. min.)	Long. (deg. min.)	Samples
RC11-237	1.6	2776	PC	0	13	-01.32	085.49	PL00116 1
RIS-29G	38.6	2230	GC	11	13	02.13	089.27	PS00121 1
RIS-29G	23.7	2230	GC	37	39	02.13	089.27	PS00122 1
RIS-30G	5.1	2500	GC	9	11	01.13	088.31	PS00123 3
RIS-32P	11.5	2770	PC	11	13	-00.09	085.59	PS00124 4
RIS-32P	19.1	2770	PC	29	31	-00.09	085.59	PS00125 4
TRI-2G	3.6	2592	GC	2	4	00.54	088.01	PS00126 1
TRI-2G	10.3	2592	GC	18	20	00.54	088.01	PS00127 1
TRI-HF-1	5.1	3003	HF	0	10	00.43	084.45	PS00128 3
TRI-HF-2	13.8	2214	HF	0	10	-01.35	084.58	PS00129 4
TRI-HF-4	20.2	2580	HF	0	10	-01.55	085.55	PS00130 5
TRI-HF-5	24.3	2688	HF	0	10	01.50	086.11	PS00131 1
TRI-HF-6	7.7	2664	HF	0	10	00.04	086.59	PS00132 2
TRI-HF-7	16.7	2768	HF	0	10	-01.53	087.01	PS00133 3
TRI-HF-1	12.7	2482	HF	0	10	00.08	087.58	PS00134 4
TRI-HF-1	15.5	2516	HF	0	10	01.54	088.02	PS00135 5
TRI-HF-1	30.7	2328	HF	0	10	04.15	088.50	PS00136 1
P-HF-6	14.0	1843	HF	0	10	07.46	082.42	PS00137 2
P-HF-7	.3	3429	HF	0	10	07.06	082.32	PS00138 3
P-HF-8	2.1	2082	HF	0	10	07.12	082.01	PS00139 4
P-HF-14	1.8	3384	HF	0	10	04.28	081.36	PS00141 1
P-HF-17	.7	3384	HF	0	10	05.38	082.51	PS00142 2
P-HF-18	.8	2246	HF	0	10	06.51	083.17	PS00143 3
P-HF-19	1.7	2512	HF	0	10	07.51	085.11	PS00144 4
P-HF-20	1.6	2857	HF	0	10	08.03	085.32	PS00145 5
P-HF-21	.8	2950	HF	0	10	08.32	085.45	PS00146 1
P-HF-22	3.4	2082	HF	0	10	09.02	084.48	PS00147 1
P-HF-23	1.1	2488	HF	0	10	08.27	084.27	PS00148 3
P-HF-24	1.8	1941	HF	0	10	08.14	083.33	PS00149 4
P-HF-26	1.2	2545	HF	0	10	08.04	084.58	PS00150 5
P-HF-27	1.2	2990	HF	0	10	07.42	085.43	PS00151 1
P-HF-28	.9	2954	HF	0	10	08.18	085.49	PS00152 2
Y69-71P	14.3	2740	PC	14	20	00.06	086.29	P000153 3
Y69-72P	27.6	2586	PC	40	47	01.01	087.27	P000156 1
Y69-73P	24.6	2707	PC	26	32	01.27	087.56	P000159 4
Y69-74P	28.2	2586	PC	26	33	02.02	088.19	P000161 1
Y69-75M2	47.2	2198	MC	34	37	03.29	089.42	P000163 4
Y69-75M2	43.8	2198	MC	16	19	03.29	089.42	P000164 4
Y69-76M1	39.8	2319	MC	19	22	01.00	092.01	P000165 5
Y69-76M2	29.2	2319	MC	17	20	01.00	092.01	P000166 1
Y69-80M1	5.3	3408	MC	15	18	-01.01	091.51	P000167 2
Y69-80M2	6.1	3408	MC	14	17	-01.01	091.51	P000168 3
Y69-83M1	10.0	3759	MC	10	13	-04.00	092.01	P000169 4
Y69-83M2	12.4	3759	MC	10	13	-04.00	092.01	P000170 5
Y69-84M1	16.6	3748	MC	14	16	-03.59	091.40	P000171 1
Y69-84M2	14.6	3748	MC	14	16	-03.59	091.40	P000172 2
Y69-86M1	3.6	3245	MC	11	14	-01.59	091.40	P000173 3
Y69-86M2	2.8	3245	MC	13	16	-01.59	091.40	P000174 4
Y69-97M1	51.5	2362	MC	19	22	00.32	091.38	P000175 5
Y69-102P	87.1	2220	PC	10	17	-01.04	085.51	P000176 1
Y69-103P	12.3	1808	PC	10	16	-00.05	082.26	P000179 4
Y69-104M	6.4	3892	MC	20	22	-02.18	081.31	P000181 1
Y69-105P	2.4	3408	PC	10	12	00.09	084.03	P000182 2
Y69-106P	26.0	2870	PC	18	24	02.59	086.33	P000184 4
Y69-107M	57.7	2716	MC	20	22	04.47	088.29	P000187 2
Y69-108P	3.5	3390	PC	10	16	04.09	085.02	P000188 3
Y69-109P	2.7	3721	PC	6	12	02.05	082.59	P000190 5
Y69-110P	23.6	3083	PC	28	34	-00.13	081.06	P000192 2
Y69-112P	.3	3848	PC	10	16	03.30	078.57	P000195 5

APPENDIX II. Specimens Per Slide

	carbonate slide							carbonate-free slide					
Sample	Pl. Foram.	Foram. Pieces	Rads	Mins.	Bent. Foram.	Nassellaria	Spumellaria	Br. Glass	Transp. Gl.	Minerals	Glauconite	Diatom	S. Spicules
1	0	5	2	3893	7	1	28	0	3	1671	1960	0	0
3	0	11	4	1760	0	4	50	0	6	2519	1854	0	1
5	2	12	3003	1638	0	182	1650	1	428	164	56	0	2
7	0	2	255	777	0	47	519	0	85	203	53	0	0
9	1	56	2031	77	0	278	1901	0	5	20	185	0	1
11	79	986	74	31	20	38	527	0	17	82	92	0	0
13	97	499	4	10	3	8	32	0	99	13	180	0	0
15	53	670	38	154	6	67	806	0	32	3	1179	0	2
17	187	363	3	6	0	12	66	0	531	231	986	0	3
19	0	0	1513	228	0	175	1860	0	8	37	280	0	4
21	0	7	2275	78	0	251	2239	0	81	15	213	0	4
23	22	802	350	17	5	834	3586	0	154	45	102	0	1
25	41	412	510	113	2	1113	4869	1	813	92	15	0	17
27	72	970	744	2	4	232	1581	0	3	2	0	0	2
29	72	796	43	13	12	12	177	0	65	6	36	0	3
31	72	317	236	24	2	3	134	0	33	16	302	0	1
33	29	177	1063	9	4	341	2347	0	5	4	15	0	0
35	13	284	650	46	12	44	538	0	3	18	37	0	2
37	9	698	7	310	12	4	18	0	4	51	1569	0	13
39	0	0	2982	1145	0	66	667	0	5	106	77	0	5
41	0	0	2289	465	0	55	647	0	6	80	38	0	0
43	0	0	84	2502	0	21	95	0	75	2808	73	0	0
45	27	409	57	19	1	172	1345	0	802	201	1754	0	5
47	25	1185	588	32	2	1509	5785	4	294	68	27	0	7
49	30	377	445	862	10	554	4030	43	2700	637	1	0	24
51	0	0	607	78	0	32	399	0	1	25	9	0	1
53	5	105	1428	24	12	450	2693	1	12	20	10	0	25
55	113	1017	20	88	10	19	135	4	229	138	2983	0	14
57	74	301	1304	132	4	1156	4309	251	418	129	106	40	10
60	57	224	106	0	0	773	2553	23	13	1	5	0	6
62	489	299	21	11	13	434	2993	22	27	1627	948	8	1306
64	1187	349	94	32	51	370	3885	1	38	854	37	1	1887
66	771	406	7	16	3	9	130	4	579	8	85	0	2
68	39	148	1836	14	0	1558	5810	3	27	12	18	0	6
70	61	1033	811	9	11	1961	7406	0	45	18	35	0	14
72	0	0	678	50	0	149	759	0	10	6	0	0	1
74	2	28	3732	821	0	1698	3952	0	979	719	9	0	15
76	5	140	105	888	131	8	101	0	59	361	301	0	0
78	0	6	2363	91	3	58	713	0	2	7	26	0	0
80	0	0	572	2273	0	6	69	0	4	236	335	0	0
82	0	4	1381	152	0	36	466	0	3	32	12	0	1
84	0	2	1167	3401	0	18	208	0	3	555	76	1	3
86	40	1496	530	36	25	155	1008	1	37	3476	549	2	12
88	394	1238	732	11	7	1236	4852	5	31	7	50	0	10
90	112	1088	1225	38	4	1819	5986	14	11	9	10	0	9
92	0	43	3841	135	2	894	5685	0	18	89	49	0	10
95	0	85	2514	2961	0	202	2256	2	1058	2122	160	0	5
97	23	431	466	1085	12	53	430	7	164	769	527	0	0
99	0	1	3399	349	0	1240	5514	2	222	207	77	0	6
101	9	155	687	421	0	688	5031	9	1237	263	0	0	13
105	3	147	2884	41	5	774	3009	9	9	16	20	0	2
107	35	891	79	6	6	361	2412	4	89	94	178	0	13
110	0	0	829	5	0	866	4030	0	7	6	0	0	1
112	0	3	1101	20	0	1346	5674	3	5	69	21	0	1
114	1	6	1602	3218	2	34	352	0	11	319	222	0	4

APPENDIX II. Specimens Per Slide

	carbonate slide					carbonate-free slide								
Sample	Pl. Foram.	Foram. Pieces	Rads	Mins.	Bent. Foram.	Nassellaria	Spumellaria	Br. Glass	Transp. Gl.	Minerals	Glauconite	Diatom	S. Spicules
116	15	283	2376	197	10	200	661	43	3	7	7	0	0
117	131	576	238	6	11	1020	3727	4	13	5	13	0	2
121	86	312	74	4	1	340	1587	18	103	3	97	0	5
122	242	644	171	4	1	832	2718	12	32	13	19	0	8
123	222	1032	2344	35	5	1023	3519	24	85	6	1	0	4
124	244	1542	1198	181	3	724	3657	13	772	8	22	0	3
125	283	519	489	2	3	608	3029	0	7	1	99	0	0
126	33	877	3116	16	4	686	2569	10	4	1	0	0	14
127	224	697	1406	4	8	307	1379	2	7	0	1	0	1
128	27	236	1656	16	2	795	2676	8	11	2	5	0	0
129	98	599	647	12	5	475	2635	10	23	12	4	0	0
130	230	726	981	12	6	546	3009	2	15	2	9	0	4
131	176	447	70	2	3	345	1968	0	9	1	33	0	0
132	31	1218	2213	24	9	974	3850	15	7	0	1	0	72
133	246	412	549	8	5	1069	4279	1	10	1	2	1	2
134	455	1199	1569	12	10	658	3303	30	14	2	1	0	7
135	127	814	1052	22	5	526	2512	7	60	6	1	0	5
136	328	964	162	3	4	523	2833	9	53	10	2	0	11
137	1	1	4	1229	0	4	48	1	49	3020	905	0	1
138	4	45	4471	792	4	457	3661	3	41	544	447	0	39
139	2	121	1513	6358	7	37	238	1	13	691	752	0	1
141	22	204	5117	94	5	1017	4152	0	50	35	14	0	13
142	1	6	2376	27	0	264	2026	1	2	9	5	0	1
143	21	459	5737	161	2	149	912	0	1	6	8	0	0
144	49	716	2005	78	2	866	3474	2	76	23	13	0	19
145	116	363	2562	39	4	1878	6338	2	71	32	37	0	14
146	1	119	3116	229	0	692	2937	3	132	112	16	0	3
147	0	203	331	2416	0	24	206	8	652	2519	1137	0	3
148	2	47	5229	2945	1	404	2201	6	225	951	289	0	1
149	1	19	3061	4060	2	82	793	8	328	2573	5	0	9
150	64	247	2759	36	2	1060	5019	4	19	72	4	1	6
151	13	72	545	26	2	771	3422	0	26	14	1	0	9
152	46	87	4095	108	4	761	3680	2	100	69	2	0	7
153	131	484	645	4	0	370	1646	1	7	6	5	0	2
156	584	1078	798	11	7	649	2716	8	13	2	4	0	0
159	369	1195	921	18	6	710	3293	9	19	4	6	0	2
161	174	163	105	10	2	315	1705	29	1217	4	1	0	4
163	243	111	50	0	0	192	1599	3	156	18	26	0	2
164	116	709	155	11	3	508	2093	3	76	73	7	0	6
165	773	758	310	82	0	290	1484	166	59	198	47	0	0
166	409	923	600	241	6	199	1287	193	44	133	11	0	4
167	80	200	2745	462	1	812	2875	313	79	302	5	1	25
168	51	311	2233	748	1	853	2833	392	96	548	8	0	16
169	85	616	3109	7	1	1218	4348	0	0	10	0	0	0
170	45	917	2186	8	3	671	2457	1	0	1	0	0	0
171	133	1202	1021	8	3	482	1767	0	0	0	0	0	0
172	67	335	539	9	1	1039	3723	0	0	5	0	0	0
173	56	421	4861	46	5	719	2151	17	2	3	0	1	3
174	21	377	3308	101	0	1354	3841	24	8	16	0	0	9
175	168	281	291	2059	4	31	168	1536	23	1362	5	0	4
176	183	163	14	1	0	374	2218	0	63	54	500	0	6
179	113	1010	1093	146	9	561	2437	4	1103	334	7	0	3
181	4	8	563	960	0	10	146	0	18	457	10	0	0
182	2	0	762	65	0	49	342	0	54	27	1	0	1
184	373	1174	179	17	5	586	2567	0	19	6	2	0	8
187	123	400	59	4	1	13	310	0	14	2	0	0	1
188	100	916	2098	30	6	318	2198	0	13	1	1	0	1
190	14	99	1541	30	1	198	1543	0	34	3	8	0	2
192	216	2150	147	509	4	217	1392	0	1452	600	242	0	1
195	0	0	699	79	0	57	361	0	53	92	0	0	6

APPENDIX IIIa. Percentages of Total Coarse Fraction

Sample	Whole Pl. Forams.	Pl. Foram. Pieces	Radiolaria	Minerals	Benthic Forams.
1	0	.1	.1	99.6	.2
3	0	.6	.2	99.2	0
5	.0	.3	64.5	35.2	0
7	0	.2	24.7	75.2	0
9	.1	2.6	93.8	3.6	0
11	6.6	82.9	6.2	2.6	1.7
13	15.8	81.4	.6	1.6	.5
15	5.4	68.3	10.0	15.7	.6
17	33.5	64.9	.5	1.1	0
19	0	0	86.9	13.1	0
21	0	.3	96.4	3.3	0
23	1.8	67.1	29.3	1.4	.4
25	3.8	38.2	47.3	10.5	.2
27	4.0	54.1	41.5	.1	.2
29	7.7	85.0	4.6	1.4	1.3
31	11.1	48.7	36.3	3.7	.3
33	2.3	13.8	82.9	.7	.3
35	1.3	28.3	64.7	4.6	1.2
37	.9	67.4	.7	29.9	1.2
39	0	0	72.3	27.7	0
41	0	0	83.1	16.9	0
43	0	0	3.3	96.8	0
45	5.3	79.7	11.1	3.7	.2
47	1.4	64.7	32.1	1.8	.1
49	1.7	21.9	25.8	50.0	.6
51	0	0	88.6	11.4	0
53	.3	6.7	90.7	1.5	.8
55	9.1	81.5	1.6	7.1	.8
57	4.1	16.6	71.8	7.3	.2
60	14.7	57.9	27.4	0	0
62	58.7	35.9	2.5	1.3	1.6
64	69.3	20.4	5.5	1.9	3.0
66	64.1	33.8	.6	1.3	.3
68	1.9	7.3	90.1	.7	0
70	3.2	53.7	42.1	.5	.6
72	0	0	93.1	6.9	0
74	.0	.6	81.4	17.9	0
76	.4	11.0	8.3	70.0	10.3
78	0	.2	95.9	3.7	.1
80	0	0	20.1	79.9	0
82	0	.3	89.8	9.9	0
84	0	.0	25.5	74.4	0
86	1.9	70.3	24.9	1.7	1.2
88	16.5	52.0	30.7	.5	.3
90	4.5	44.1	49.7	1.5	.2
92	0	1.1	95.5	3.4	.1
95	0	1.5	45.2	53.3	0
97	1.1	21.4	23.1	53.8	.6
99	0	.0	90.7	9.3	0
101	.7	12.2	54.0	33.1	0
105	.1	4.8	93.6	1.3	.2
107	8.8	82.7	7.3	.6	.6
110	0	0	99.4	.6	0
112	0	.3	97.9	1.8	0
114	.0	.1	33.2	66.6	.0
116	.5	9.8	82.5	6.8	.3
117	13.6	59.9	24.7	.6	1.1
121	18.0	65.4	15.5	.8	.2
122	22.8	60.6	16.1	.4	.1
123	6.1	28.4	64.4	1.0	.1
124	7.7	48.7	37.8	5.7	.1

APPENDIX IIIa. Percentages of Total Coarse Fraction

Sample	Whole Pl. Forams.	Pl. Foram. Pieces	Radiolaria	Minerals	Benthic Forams.
125	21.8	40.0	37.7	.1	.2
126	.8	21.7	77.0	.4	.1
127	9.6	29.8	60.1	.2	.3
128	1.4	12.2	85.5	.8	.1
129	7.2	44.0	47.5	.9	.4
130	11.9	37.1	50.2	.6	.3
131	25.2	64.0	10.0	.3	.4
132	.9	34.8	63.3	.7	.3
133	20.2	33.8	45.0	.7	.4
134	14.0	37.0	48.3	.4	.3
135	6.3	40.3	52.1	1.1	.3
136	22.5	66.0	11.1	.2	.3
137	.1	.1	.3	99.5	0
138	.1	.9	84.1	14.9	.1
139	.0	1.5	18.9	79.5	.1
141	.4	3.8	94.0	1.7	.1
142	.0	.3	98.6	1.1	0
143	.3	7.2	89.9	2.5	.0
144	1.7	25.1	70.3	2.7	.1
145	3.8	11.8	83.1	1.3	.1
146	.0	3.4	89.9	6.6	0
147	0	6.9	11.2	81.9	0
148	.0	.6	63.6	35.8	.0
149	. .0	.3	42.8	56.8	.0
150	2.1	7.9	88.8	1.2	.1
151	2.0	10.9	82.8	4.0	.3
152	1.1	2.0	94.3	2.5	.1
153	10.4	38.3	51.0	.3	0
156	23.6	43.5	32.2	.4	.3
159	14.7	47.6	36.7	.7	.2
161	38.3	35.9	23.1	2.2	.4
163	60.2	27.5	12.4	0	0
164	11.7	71.3	15.6	1.1	.3
165	24.5	49.8	20.4	5.4	0
166	18.5	42.4	27.5	11.1	.3
167	2.3	5.7	78.7	13.3	.0
168	1.5	9.3	66.8	22.4	.0
169	2.2	16.1	81.4	.2	.0
170	1.4	29.0	69.2	.3	.1
171	5.6	50.8	43.1	.3	.1
172	7.1	35.2	56.7	.9	.1
173	1.0	7.8	90.2	.9	.1
174	.6	9.9	86.9	2.7	0
175	6.0	10.1	10.4	73.4	.1
176	50.7	45.2	3.9	.3	0
179	5.0	42.5	46.0	6.1	.4
181	.3	.5	36.7	62.5	0
182	.2	0	91.3	7.8	0
184	21.3	67.2	10.2	1.0	.3
187	21.0	68.1	10.1	.7	.2
188	3.2	29.1	66.6	.9	.2
190	.8	5.9	91.4	1.8	.1
192	7.1	71.0	4.9	16.8	.1
195	0	0	89.8	10.1	0

APPENDIX IIIb. Percentages of Carbonate-Free Coarse Fraction

Sample	Nassellaria	Spumellaria	Br. Glass	Transp. Gl.	Minerals	Glauconite	Diatom	S. Spicule
1	.3	.8	0	.1	45.5	53.5	0	0
3	.1	1.1	0	.1	56.8	41.8	0	.0
5	7.3	66.4	.0	17.2	6.6	2.3	0	.1
7	5.2	57.2	0	9.4	22.4	5.8	0	0
9	11.6	79.5	0	.2	.8	7.7	0	.0
11	5.0	69.7	0	2.3	10.9	12.2	0	0
13	2.4	9.6	0	29.8	3.9	54.2	0	0
15	3.2	36.5	0	1.5	.1	56.4	0	.1
17	.7	3.0	0	29.0	12.6	53.9	0	.2
19	7.4	78.7	0	.3	1.6	11.8	0	.2
21	6.9	79.9	0	2.9	.5	7.6	0	.1
23	17.7	75.9	0	3.3	.9	2.2	0	.0
25	16.1	70.4	.0	11.3	1.3	.2	0	.3
27	12.8	86.9	0	.2	.1	0	0	.1
29	4.0	59.2	0	21.7	2.0	12.0	0	1.0
31	.6	27.4	0	6.8	3.3	61.8	0	.2
33	12.6	86.5	0	.2	.1	.6	0	0
35	6.8	83.8	0	.5	2.8	5.8	0	.3
37	.2	1.1	0	.2	3.1	94.6	0	.8
39	7.1	72.0	0	.5	11.4	8.3	0	.5
41	6.7	78.3	0	.7	9.7	4.6	0	0
43	.7	3.1	0	2.4	91.4	2.4	0	0
45	4.0	31.4	0	18.7	4.7	41.0	0	.1
47	19.6	75.2	.1	3.9	.9	.3	0	.1
49	6.9	50.4	.5	33.8	8.0	.0	0	.3
51	6.8	85.4	0	.2	5.3	1.9	0	.2
53	14.0	83.3	.0	.4	.6	.3	0	.8
55	.5	3.8	.1	6.5	3.9	84.7	0	.4
57	18.9	67.1	3.9	6.5	2.0	1.6	.6	.2
60	22.8	75.7	.7	.4	.0	.1	0	.2
62	5.9	40.6	.3	.4	22.1	12.9	.1	17.7
64	5.2	54.9	.0	.5	12.1	.5	.0	26.7
66	1.1	15.9	.5	70.9	1.0	10.4	0	.2
68	21.0	78.2	.0	.4	.2	.2	0	.1
70	20.7	78.1	0	.5	.2	.4	0	.1
72	16.1	82.1	0	1.1	.6	0	0	.1
74	13.7	72.4	0	7.9	5.8	.1	0	.1
76	1.0	12.2	0	7.1	43.5	35.3	0	0
78	7.2	88.5	0	.3	.9	3.2	0	0
80	.9	10.6	0	.6	36.3	51.5	0	0
82	6.6	84.7	0	.6	5.8	2.2	0	.2
84	2.1	24.1	0	.3	64.2	8.8	.1	.3
86	3.0	19.2	.0	.7	66.3	10.5	.0	.2
88	20.0	78.4	.1	.5	.1	.8	0	.2
90	23.1	76.2	.2	.1	.1	.1	0	.1
92	13.3	84.3	0	.3	1.3	.7	0	.1
95	3.5	38.9	.0	18.2	36.5	2.8	0	.1
97	2.7	22.0	.4	8.4	39.4	27.0	0	0
99	17.1	75.9	.0	3.0	2.8	1.1	0	.1
101	9.5	69.5	.1	17.1	3.6	0	0	.2
105	20.2	78.4	.2	.2	.4	.5	0	.1
107	11.5	79.5	.1	2.8	3.0	5.7	0	.4
110	17.6	82.1	0	.1	.1	0	0	.0
112	18.9	79.7	.0	.1	1.0	.3	0	.0
114	7.6	37.4	0	1.2	37.9	23.6	0	.4
116	21.7	71.8	4.7	.3	.8	.8	0	0
117	21.7	77.9	.1	.3	.1	.3	0	.0
121	15.8	73.7	.8	4.6	.1	4.5	0	.2
122	22.4	74.8	.3	.9	.4	.5	0	.2
123	21.4	75.5	.5	1.6	.1	.0	0	.1
124	13.9	79.3	.7	14.9	.1	.4	0	.1

APPENDIX IIIb. Percentages of Carbonate-Free Coarse Fraction

Sample	Nassellaria	Spumellaria	Br. Glass	Transp. Gl.	Minerals	Glauconite	Diatom	S. Spicule
125	16.2	80.9	0	.2	.0	2.6	0	0
126	20.9	78.2	.3	.1	.0	0	0	.4
127	18.1	81.3	.1	.4	0	.1	0	.1
128	22.7	76.5	.2	.3	.1	.1	0	0
129	15.0	83.4	.3	.7	.4	.1	0	0
130	15.2	83.9	.1	.4	.1	.3	0	.1
131	14.6	83.5	0	.4	.0	1.4	0	0
132	19.8	78.3	.3	.1	0	.0	0	1.5
133	19.9	79.8	.0	.2	.0	.0	.0	.0
134	16.4	82.3	.8	.3	.1	.0	0	.2
135	16.9	80.6	.2	1.9	.2	.0	0	.2
136	15.2	82.3	.3	1.5	.3	.1	0	.3
137	.1	1.2	.0	1.2	75.0	22.5	0	.0
138	3.8	70.5	.1	.8	16.5	8.6	0	.8
139	2.1	13.7	.1	.6	39.9	43.4	0	.1
141	19.3	78.6	0	.9	.7	.3	0	.3
142	11.4	87.3	.0	.1	.4	.2	0	.0
143	13.9	84.8	0	.1	.6	.7	0	0
144	19.4	77.7	.0	1.7	.5	.3	0	.4
145	21.2	77.1	.0	.8	.4	.4	0	.2
146	17.8	75.4	.1	3.4	2.9	.4	0	.1
147	.5	4.5	.2	14.3	55.4	25.0	0	.1
148	9.0	54.0	.1	5.5	23.3	7.1	0	.0
149	2.2	20.9	.2	3.6	67.8	.1	0	.2
150	17.1	81.2	.1	.3	1.2	.1	.0	.1
151	19.2	80.7	0	.6	.3	.0	0	.2
152	16.5	79.6	.0	2.2	1.5	.0	0	.1
153	18.2	80.3	.1	.3	.3	.3	0	.1
156	19.1	80.1	.2	.4	.1	.1	0	0
159	17.6	81.4	.2	.5	.1	.1	0	.1
161	9.6	52.1	.9	37.2	.1	.0	0	.1
163	9.6	85.1	.1	7.8	.9	1.3	0	.1
164	18.4	75.7	.1	2.8	2.6	.3	0	.2
165	12.0	56.1	7.4	2.6	8.8	2.1	0	0
166	10.6	68.8	10.3	2.3	7.1	.6	0	.2
167	19.4	65.2	7.1	1.8	6.8	.1	.0	.6
168	18.0	59.7	8.3	2.0	11.5	.2	0	.3
169	21.8	78.0	0	0	.2	0	0	0
170	21.4	78.5	.0	0	.0	0	0	0
171	21.4	78.6	0	0	0	0	0	0
172	21.8	78.1	0	0	.1	0	0	0
173	24.8	74.3	.6	.1	.1	0	.0	.1
174	25.8	73.1	.5	.1	.3	0	0	.2
175	1.0	5.4	49.1	.7	43.5	.2	0	.1
176	11.6	63.0	0	2.0	1.7	15.6	0	.2
179	12.5	54.8	.1	24.8	7.5	.2	0	.1
181	1.5	22.8	0	2.8	71.3	1.6	0	0
182	10.3	72.2	0	11.4	5.7	.2	0	.2
184	13.4	80.5	0	.6	.2	.1	0	.3
187	3.8	91.2	0	4.1	.5	0	0	.3
189	12.6	86.8	0	.5	.0	.0	0	.0
190	11.1	86.3	0	1.9	.2	.4	0	.1
192	5.6	35.7	0	37.2	15.4	6.2	0	.0
193	5.3	80.5	0	5.0	8.5	0	0	.6

APPENDIX IV

Sample Preparation and Counting Procedure

Undisturbed tops of gravity and some piston cores were obtained from the collections of Lamont, Scripps and OSU. Locations of the cores, bottom depths and sampling intervals within the cores are listed in Appendix I.

At OSU, the samples were washed and sieved through a 62 μ mesh. The coarser-than-62 μ fraction was dried in an oven at 100° C and subsequently split once, with a microsplitter. One split was further subdivided until only enough material was left to make one slide (carbonate slide). The other split was warmed in buffered acetic acid of pH = 5, to dissolve the carbonate components but preserve all the delicate radiolaria intact. During the splitting operation, care was taken to avoid air currents and the splitters were tamped on a hard surface until all the radiolaria sticking to the walls of the splitter fell into the buckets underneath.

Once the material for the carbonate slide had been isolated, it was transferred to 1 ml beakers. These were one-fourth filled with water using a squeeze bottle with a very fine nozzle. The water was used to ensure an even distribution of the material once it was dumped onto the slide, and to prevent the light radiolaria from flying away during the transfer to the slide. The microscope glass slides had been previously marked with the sample identification and had been placed on a hot plate at about 100° C. To avoid spreading of the sample on the glass slide, a frame of silicone grease was applied with a carved-out eraser that had the same dimensions as the cover slip. This frame also allowed the addition of enough balsam to completely cover the thick planktonic foraminifera.

Once on the slide, the water containing the sediment was allowed to evaporate. Additional washings of the beaker onto the slide ensured that all the sample was transferred. Immediately after complete evaporation of the water, balsam slightly diluted with xylene was added to the slide until all foraminifera were covered. The slide was allowed to sit on the hot plate for a few seconds so that the air bubbles trapped in the foraminiferal tests could escape. A cover slip was then applied with very little pressure. The most fragile globigerinids survived this treatment without breaking. Since original foraminiferal fragments in the sediment were to be counted, this was an important consideration. The finished slide was put into an oven at 50° C for hardening of the balsam for at least 24 hours.

The split used in the carbonate-free slide was inspected with a binocular microscope after 12 hours in warm acetic acid with periodic stirring. If all the carbonate had been removed, the sample was transferred to a 62 μ sieve, washed to remove all the acid and then dried. It was then split until just enough sample remained for making one slide and processed in the same way as the carbonate slide.

The contents of the slides were identified and counted using a Leitz binocular petrographic microscope. All grains present under the cover slip were counted. Planktonic foraminifera were considered whole when the proloculus was present even if parts of the later chambers were missing. An occasional foraminifer that was broken during mounting of the cover slip was easy to identify. The pieces lay close together and were radially distributed. These pieces were counted as one whole foraminifer.

Only four samples contained enough heavy minerals for an effective separation. The carbonate-free splits were separated in bromoform ($\rho = 2.89$) by standard procedure (Tickell, 1965). The heavy minerals were mounted on slides with Aroclor ($n = 1.66$) and were identified with a Zeiss petrographic microscope.

APPENDIX V. Bottom Water Hydrographic Data

Ship	Lat.	Long. (W)	Depth Cast	Temp.	Salin.	Dens.	Pot. T.	Pot. D.	Depth Bottom
VE	9.20	89.05	3492	1.90	0	0	1.79	0	3488
TT	8.00	89.28	2905	1.82	34.675	27.76	1.60	27.77	0
EX	8.57	88.26	2455	1.85	34.670	27.75	1.67	27.77	2964
RC	8.33	88.03	3334	1.86	34.647	27.73	1.59	27.75	3372
TT	9.09	88.59	3019	1.85	34.658	27.74	1.62	27.76	3310
VE	9.43	88.00	3169	1.84	0	0	1.75	0	3169
TT	8.00	87.00	3011	1.83	34.674	27.76	1.60	27.77	3164
M4	8.46	86.17	3120	1.85	34.665	27.75	1.61	27.77	3091
TT	9.54	86.27	4496	2.00	34.676	27.75	1.59	27.78	4518
	9.02	86.50	2500	0	34.670	0	0	0	3110
OC	9.23	86.26	3226	1.86	34.675	27.76	1.60	27.77	3220
TT	8.58	85.57	2460	1.85	34.668	27.75	1.67	27.76	3102
HN	9.57	81.36	2273	4.04	0	0	3.95	0	2924
RC	7.17	92.03	3538	1.87	34.671	27.75	1.58	27.77	2375
HO	7.15	88.46	2888	1.83	0	0	1.75	0	3438
V5	7.06	88.04	2448	1.82	34.670	27.75	1.64	27.77	0
V5	7.10	88.12	2936	1.85	34.680	27.76	1.62	27.78	3410
VE	7.55	86.00	3080	1.86	0	0	1.77	0	3079
VF	7.05	85.55	2855	1.82	0	0	1.75	0	2859
RH	7.01	82.22	2382	2.04	34.660	27.73	1.86	27.74	3109
DA	7.30	79.19	2500	2.09	34.640	27.71	1.90	27.72	2550
	7.06	79.55	3000	2.02	34.630	27.71	1.78	27.73	3548
DA	7.07	78.41	2900	2.03	34.670	27.74	1.80	27.76	3150
HN	7.16	78.24	2183	2.18	34.690	27.74	2.02	27.76	2300
OC	7.02	78.50	3693	2.02	34.672	27.74	1.71	27.76	3685
	7.16	78.30	3500	2.02	34.650	27.72	1.73	27.75	3650
RH	7.01	78.49	3368	1.98	34.680	27.75	1.71	27.77	3475
SB	6.04	89.57	2907	1.84	34.650	27.74	1.62	27.75	3603
VF	6.53	83.16	2272	2.13	0	0	2.08	0	2267
OC	6.00	82.35	4713	2.20	34.672	27.73	1.76	27.76	4698
OC	6.15	82.50	3509	2.10	34.675	27.74	1.81	27.76	3550
HN	6.56	82.00	2407	2.10	34.670	27.73	1.92	27.75	2700
DA	6.49	80.25	2900	2.02	34.670	27.74	1.79	27.76	3140
CN	6.32	80.04	3063	2.04	34.620	27.70	1.80	27.72	3583
6A	6.39	80.32	3409	2.04	34.670	27.74	1.76	27.76	3490
YQ	6.43	79.45	3306	2.02	34.675	27.74	1.75	27.76	3333
RH	6.58	79.57	2359	2.18	34.670	27.73	2.00	27.74	3054
M4	6.56	79.14	3270	1.99	34.660	27.73	1.73	27.75	3200
OC	6.12	78.54	3189	1.98	34.674	27.75	1.73	27.76	3190
RC	5.16	87.57	2528	1.91	34.667	27.75	1.72	27.76	2550
YQ	5.09	85.00	2676	2.04	34.663	27.73	1.84	27.75	2703
OC	5.29	83.58	3435	2.09	34.673	27.74	1.81	27.76	3439
RH	5.04	83.38	2908	2.05	34.670	27.74	1.82	27.75	3295
CN	5.59	82.56	3231	2.10	34.630	27.70	1.84	27.72	3324
RH	5.01	82.24	2639	2.01	34.680	27.75	1.81	27.76	2995
YQ	5.09	82.38	2463	2.06	34.638	27.71	1.88	27.72	2437
OC	5.28	81.11	3700	2.04	34.675	27.74	1.73	27.77	3704
YQ	5.29	81.13	3702	2.09	34.671	27.73	1.78	27.76	3768
RH	5.01	81.08	3489	2.01	34.680	27.75	1.72	27.77	3658
RC	5.18	80.30	2978	2.00	34.672	27.74	1.77	27.76	3786
OC	5.31	80.08	3026	1.99	34.675	27.75	1.75	27.76	3008
HO	5.43	80.31	2665	1.96	34.640	27.72	1.76	27.73	2926
YQ	5.15	80.18	3603	2.03	34.657	27.73	1.73	27.75	3637
RH	5.02	79.57	2567	2.05	34.670	27.74	1.86	27.75	3091
RH	5.02	78.44	3325	1.97	34.700	27.77	1.70	27.79	3436

APPENDIX V. Bottom Water Hydrographic Data

Ship	Lat.	Long. (W)	Depth Cast	Temp.	Salin.	Dens.	Pot. T.	Pot. D.	Depth Bottom
YQ	5.00	78.00	3830	0	34.676	0	0	0	0
RC	4.41	91.58	3393	1.84	34.678	27.76	1.57	27.78	3270
YQ	4.47	88.26	2697	1.84	34.671	27.75	1.64	27.77	2716
YQ	4.06	85.00	3365	2.13	34.669	27.73	1.85	27.75	3390
OC	4.26	84.22	3849	2.14	34.670	27.73	1.81	27.76	3847
RH	4.53	84.54	2280	2.05	0	0	2.00	0	2287
V5	4.21	84.12	2918	2.08	34.660	27.73	1.85	27.74	0
OC	4.46	82.12	3847	2.07	34.676	27.74	1.74	27.77	3857
OC	4.42	82.52	3674	2.11	34.674	27.74	1.80	27.76	3647
OC	4.59	81.05	3752	2.06	34.675	27.74	1.74	27.76	3757
OC	4.34	78.21	3690	1.99	34.674	27.74	1.68	27.77	3684
VE	4.25	78.20	3755	2.03	0	0	1.90	0	3755
YQ	3.00	92.00	2537	1.85	34.668	27.75	1.66	27.76	2410
YQ	3.28	89.43	2161	2.01	34.658	27.73	1.86	27.74	2198
YQ	3.00	85.39	2991	2.07	34.662	27.73	1.83	27.75	3020
YQ	3.59	84.57	3073	2.07	34.665	27.73	1.83	27.75	3045
YQ	3.00	84.59	3001	2.07	34.654	27.72	1.83	27.74	3030
RH	3.04	83.42	2620	2.03	34.670	27.74	1.83	27.75	2730
CN	3.46	81.37	2264	2.17	0	0	2.11	0	2264
RH	3.05	81.06	2365	2.06	34.680	27.74	1.89	27.75	2895
YQ	3.24	79.00	3845	2.04	34.676	27.74	1.71	27.77	3848
YQ	3.50	79.40	3918	2.05	34.677	27.74	1.71	27.77	3950
YQ	2.59	90.00	2122	2.18	34.648	27.71	2.03	27.72	2140
YQ	2.05	89.29	2247	2.13	34.660	27.72	1.97	27.74	0
RC	2.02	88.03	2479	2.07	34.670	27.74	1.88	27.75	2454
YQ	2.02	88.18	2480	2.10	34.660	27.73	1.91	27.74	2586
YQ	2.58	86.32	2802	2.08	34.660	27.73	1.86	27.74	2870
RH	2.55	86.16	2702	2.04	34.660	27.73	1.83	27.75	2835
YQ	2.59	86.30	2800	2.05	34.657	27.73	1.83	27.74	2811
RC	2.56	85.00	3096	2.09	34.660	27.73	1.84	27.74	0
RH	2.58	84.58	2828	2.05	34.680	27.74	1.83	27.76	3017
YQ	2.01	84.36	3285	2.07	34.679	27.74	1.80	27.76	3127
OC	2.36	83.35	3465	2.07	34.670	27.74	1.78	27.76	3460
YQ	2.00	83.51	3279	2.05	34.664	27.73	1.78	27.75	3270
YQ	2.05	82.57	3697	2.06	34.670	27.74	1.75	27.76	3721
CN	2.54	80.02	2314	2.18	34.910	27.92	2.01	27.93	4880
YQ	2.00	80.28	4228	2.08	34.668	27.73	1.70	27.76	4240
OC	2.50	80.08	4879	2.16	34.675	27.73	1.70	27.77	4850
OC	2.36	79.26	3539	1.96	34.672	27.75	1.67	27.77	3534
YQ	1.30	93.00	2595	1.82	34.664	27.75	1.63	27.76	2580
YQ	1.00	92.00	2327	1.97	34.657	27.73	1.80	27.75	2319
YQ	1.09	90.01	2016	2.22	34.649	27.71	2.07	27.72	2067
YQ	1.30	88.15	2583	2.06	34.661	27.73	1.86	27.74	2535
YQ	1.00	87.25	2384	2.06	34.662	27.73	1.88	27.74	2586
YQ	1.28	87.54	2599	2.07	34.665	27.73	1.87	27.75	2707
RH	1.03	87.25	2530	2.08	34.680	27.74	1.89	27.76	2645
YQ	1.58	86.30	2840	2.08	34.675	27.74	1.86	27.76	2868
YQ	1.00	86.30	2620	2.06	34.656	27.72	1.86	27.74	2640
AL	1.45	86.14	2464	2.05	34.690	27.75	1.87	27.77	2770
RH	1.01	86.14	2587	2.07	34.720	27.78	1.87	27.79	2560
YQ	1.59	85.29	2743	2.05	34.665	27.73	1.84	27.75	2680
HO	1.01	84.59	2800	2.03	0	0	1.95	0	2880
RH	1.04	84.55	2828	2.04	34.690	27.75	1.82	27.77	2880
OC	1.29	84.14	3319	2.04	34.674	27.74	1.77	27.76	3303
YQ	1.00	83.51	3410	2.05	34.656	27.73	1.77	27.75	3325
OC	1.01	83.28	3402	2.05	34.672	27.74	1.77	27.76	3364
RH	1.07	82.29	3033	2.00	34.670	27.74	1.76	27.76	3145
OC	1.28	82.29	2975	2.01	34.673	27.74	1.78	27.76	2967
RH	1.03	81.10	2799	2.01	34.670	27.74	1.79	27.76	2972
YQ	1.01	80.46	2511	2.06	34.665	27.73	1.87	27.75	2487
OC	1.36	80.18	3306	1.90	34.670	27.75	1.63	27.77	3347
YQ	.30	91.39	2741	1.85	34.674	27.76	1.64	27.77	2362

APPENDIX V. Bottom Water Hydrographic Data

Ship	Lat.	Long. (W)	Depth Cast	Temp.	Salin.	Dens.	Pot. T.	Pot. D.	Depth Bottom
RC	.01	87.57	2425	2.09	34.663	27.73	1.91	27.74	0
YO	.04	86.29	2737	2.03	34.666	27.74	1.82	27.75	2740
CO	.10	86.20	2470	2.06	34.669	27.74	1.88	27.75	2850
YO	0	86.30	2716	2.00	34.664	27.74	1.79	27.75	2720
V5	.25	85.43	2442	2.09	34.660	27.73	1.91	27.74	0
YO	.59	85.30	2670	2.06	34.667	27.73	1.86	27.75	2650
OC	.18	84.49	3057	2.36	34.672	27.71	2.11	27.73	3070
YO	.06	84.03	3395	2.09	34.672	27.74	1.81	27.76	3408
YO	0	83.51	3119	2.04	34.659	27.73	1.79	27.75	2990
RH	.59	83.42	3320	2.04	34.670	27.74	1.77	27.76	3292
OC	.58	81.46	3493	2.19	34.670	27.73	1.90	27.75	3528
RC	.18	81.57	2536	2.03	34.660	27.73	1.84	27.74	2633
YO	.15	81.34	2056	2.22	34.653	27.71	2.07	27.72	2100
YO	.11	80.53	3700	1.94	34.662	27.74	1.63	27.76	3466
OC	-0.17	80.52	3720	1.93	34.678	27.75	1.62	27.78	3728
YO	-0.12	81.05	3165	1.82	34.683	27.76	1.57	27.78	3083
OC	-0.17	81.07	3098	1.84	34.675	27.76	1.60	27.77	3042
YO	-0.26	81.11	2730	1.78	34.676	27.76	1.58	27.78	2770
RC	-0.47	84.55	2886	2.05	34.672	27.74	1.82	27.76	3008
OC	-0.47	85.36	2458	2.04	34.668	27.74	1.86	27.75	2408
YO	-0.59	85.26	2321	2.05	34.655	27.72	1.88	27.74	2305
YO	-0	85.30	3352	2.08	34.666	27.73	1.81	27.75	3330
YO	-0.41	85.31	2669	2.03	34.662	27.73	1.83	27.75	2595
YO	-0	88.15	2323	2.08	34.662	27.73	1.91	27.74	2304
RC	-0.59	92.00	3157	1.88	34.679	27.76	1.63	27.78	3369
RH	-1.10	81.24	2700	1.77	34.660	27.75	1.57	27.76	2743
YO	-1.56	81.32	2957	1.77	34.672	27.76	1.54	27.78	0
YO	-1.07	81.21	2963	1.77	34.677	27.76	1.54	27.78	0
RH	-1.10	81.28	2676	1.80	34.680	27.76	1.60	27.78	2695
RH	-1.11	81.28	2700	1.83	34.680	27.76	1.63	27.78	2688
RH	-1.09	81.29	2135	2.21	0	0	2.16	0	2393
YO	-1.58	83.50	2174	2.15	34.657	27.72	1.99	27.73	2170
YO	-1.09	85.20	2265	2.01	34.670	27.74	1.85	27.75	0
RH	-1.21	86.11	2500	1.87	34.680	27.76	1.69	27.77	2505
RH	-1.33	87.42	2694	1.78	0	0	1.71	0	2670
TT	-1.55	88.42	2834	1.74	34.688	27.77	1.53	27.79	2928
YO	-1.00	92.00	3468	1.83	34.675	27.76	1.55	27.78	3408
YO	-1.30	93.00	3367	1.80	34.678	27.76	1.53	27.78	3340
WS	-2.11	81.53	3000	1.75	34.670	27.76	1.52	27.78	3109
YO	-2.11	81.29	3848	1.82	34.686	27.77	1.50	27.79	3892
YO	-2.42	81.47	3291	1.80	34.674	27.76	1.54	27.78	3245
YO	-2.42	81.34	4322	1.76	34.684	27.77	1.38	27.80	3245
YO	-2.11	81.47	2904	1.80	34.670	27.76	1.58	27.77	3050
YO	-2.23	82.00	2652	1.77	34.677	27.76	1.57	27.78	2635
YO	-2.10	83.00	2562	1.84	34.672	27.75	1.65	27.77	2525
TT	-2.44	84.35	2807	1.75	34.677	27.77	1.54	27.78	2926
HO	-2.06	84.14	2489	1.92	34.666	27.74	1.74	27.76	2531
YO	-2.00	85.30	2510	1.87	34.664	27.75	1.69	27.76	2440
YO	-2.59	85.30	3209	1.79	34.678	27.76	1.54	27.78	3165
AO	-2.19	86.06	2953	1.79	34.870	27.92	1.56	27.93	3200
YO	-2.00	86.30	2855	1.77	34.673	27.76	1.55	27.78	2822
AL	-2.52	89.50	3126	1.86	0	0	1.77	0	3230
YO	-2.09	90.00	3173	1.78	34.662	27.75	1.53	27.77	3135
YO	-2.00	91.40	3208	1.81	34.678	27.76	1.56	27.78	3245
RC	-3.06	82.01	3027	1.78	34.663	27.75	1.55	27.77	3075
AO	-3.52	82.28	2830	1.79	34.677	27.76	1.58	27.78	3800
AO	-3.05	84.06	2682	1.80	34.674	27.76	1.60	27.77	3180
V5	-3.57	85.49	2755	1.84	34.690	27.77	1.63	27.78	0
RC	-3.47	88.03	3445	1.80	34.679	27.76	1.52	27.78	3545
YO	-3.00	89.13	3353	1.81	34.672	27.76	1.54	27.78	3310
YO	-3.01	92.00	3507	1.81	34.676	27.75	1.53	27.78	3456

APPENDIX VI

Location of Hydrographic Stations used in the sections of Figure 3.

Transect	Station	NODC ID	Lat.	W Long.	Bottom Depth
CD	1	EX 310864	8.57	88.26	2964
CD	2	RC 311166	8.33	88.03	3372
CD	3	TT 311504	8.00	87.00	3164
CD	4	YPT 29	6.18	85.12	1700
CD	5	OC 311681	5.29	83.58	3439
CD	6	RH 310675	5.04	83.38	3295
CD	7	OC 311681	4.42	82.52	3647
GH	1	YTP 107	4.47	88.26	2750
GH	2	YPT 34	3.57	87.34	1600
GH	3	YTP 106	2.58	86.32	2810
IJ	1	YTT 75	3.28	89.43	2200
IJ	2	YPT 37	2.34	89.01	2000
IJ	3	YTT 75	2.02	88.18	2500
IJ	4	YTT 73	1.28	87.54	2600
IJ	5	RH 310675	1.03	87.25	2645
QR	1	YQ 714/41	0.59	85.30	2650
QR	2	YQ 714/39	0.00	85.30	3330
QR	3	YQ 714/49A	0.41S	85.31	2595
QR	4	YQ 714/37	0.59S	85.26	2305
QR	5	YQ 714/35	2.00S	85.30	2440
QR	6	YQ 714/33	2.59S	85.30	3165
QR	7	V5 311621	3.57S	85.49	3500

APPENDIX VII

Processing of Hydrographic Data

The parameters used to define the physical oceanographic conditions in the basin were potential temperature and potential density. Potential temperature was obtained by applying the formula of Fofonoff (1962) to the temperatures measured by reversing thermometers from hydrocasts. Potential density was obtained by inserting potential temperatures and salinities in the Sigma-T formula of Cox _et al._ (1970).

The temperatures used in tracing bottom water circulation were measured as near to the bottom as possible. The station locations and maximum depth of casts are given in Appendix V. Stations over local topographic highs were not taken into consideration. The topography is based on the bathymetric map of van Andel _et al._ (1971a) and on a small area on the central Carnegie Ridge, conducted by Malfait and Baumgartner (unpublished data surveyed during YALOC-71, Leg 3).

In the potential density cross sections (Figure 3), topographic details are included only where they affect the interpretation of the isopycnals.